UNIVERSITY OF TURKU

Directing Cell Front-Rear Polarization and Migration with Dynamic Micropatterning

– Protein Coating and Cell Type Specific Differences

Institute of Biomedicine
Master's Degree Programme in Biomedical Sciences
Drug Discovery and Development
Master's thesis

Author(s):
Karla Saukkonen

Supervisor(s):
Johanna Ivaska, PhD
Aleksi Isomursu, PhD

01.10.2024
Turku

UNIVERSITY OF TURKU

Master's thesis

Subject: Drug Discovery and Development
Author(s): Karla Saukkonen
Title: Directing Cell Front-Rear Polarization and Migration with Dynamic Micropatterning – Protein Coating and Cell Type Specific Differences
Supervisor(s): Johanna Ivaska, PhD; Aleksi Isomursu, PhD
Number of pages: 67 pages
Date: 01.10.2024

Cell migration is fundamental in many physiological processes, including tissue repair and immune responses, as well as in pathological processes including chronic inflammation and cancer metastasis. Front-rear polarization and cell adhesion are essential steps of cell migration. Understanding the steps and mechanisms that regulate cell polarization and migration can enable designing therapeutic strategies that target these events.

Micropatterning, i.e., controlling the distribution of surface molecules with microscale resolution, can be used to create patterns of adhesive surface areas and to control the placement and shape of living cells on the surface. Compared to traditional cell culture, single cell micropatterning reduces the variability between the cells and allows easy normalization of the cells, also between experiments.

With dynamic micropatterning, areas between the attached cells, which are biologically inert, can be made permissive for cell-substrate adhesion, and thus attached cells can be released to migrate and create new cell-substrate and cell-cell connections in controlled and standardized manner. The development of dynamic micropatterns has enabled enjoying the benefits of micropatterning, while studying dynamic processes such as cell polarization and migration.

In this thesis project we introduced a novel low-cost, easily accessible method for producing dynamic micropatterns by utilizing biotin-streptavidin binding. Experiments on coating efficacy, specificity and biocompatibility were performed to validate the method for use in academic cell research laboratories.

It has been earlier demonstrated that asymmetric micropatterns, including crossbow-shaped micropatterns, can control and guide cell front-rear polarity. [Jiang et al., 2005; Théry et al., 2006] In this thesis we investigated whether the geometric control of cell polarity is influenced by the specific adhesive substrate the cells are adhering to. Indeed, immunofluorescence imaging of fixed cells on micropatterns revealed substrate-dependent differences in U-251 MG cell polarization.

By live-imaging the dynamics of the cell front-rear polarization of U-251 MG cells on fibronectin and an anti-integrin antibody mAb13 -coated crossbow-shaped micropatterns, it was observed that although fibronectin was better at controlling the direction of the front-rear polarization, the direction of the front-rear polarization stayed rather static in both groups.

Finally, the novel method of dynamic micropatterning was used to determine whether cell behavior at the onset of migration is affected by the adhesive ligand. Streptavidin-conjugated fibronectin allowed instant modification of the biotinylated surface, and U-251 MG cells rapidly migrated from both substrates to the newly modified areas. Again mAb13-coated micropatterns did not control the direction of the front-rear polarization as effectively as fibronectin-coated micropatterns, but in both groups most cells did spread and migrate towards the broader edge of the micropattern with more adhesive area.

Key words: cell front-rear polarization, cell migration, dynamic micropatterning

Table of contents

1 Introduction

1.1 Cell adhesion and polarization in directed cell migration

Cell migration, the movement produced by the cells to go from one place to another, is essential for many fundamental physiological processes, such as embryonic development, tissue repair, and immune response, but also in central role in many pathological processes such as chronic inflammation and cancer metastasis [Sarkar et al., 2020; SenGupta et al., 2021].

Migrating cells need to constantly interact with their environment, the extracellular matrix (ECM), using adhesion receptors, such as integrins, which mediate bidirectionally cell-ECM signaling through the plasma membrane by sensing and responding to different intra- and extracellular cues through specialized adhesion complexes [Conway and Jacquemet, 2019]. Various chemical and mechanical cues, including geometry of the microenvironment, can modulate cell polarization and migration behavior. Front-rear polarization, a clear functional distinction between the cell leading edge and the trailing rear, enables directed cell migration, and can alone encourage spontaneous cell migration even in absence of external cues [Jiang et al., 2005].

1.1.1 Cell body on the move - different migration strategies

Cell migration is a tightly controlled process, happening in constant interaction with the surrounding ECM and influenced by neighboring cells. It requires highly dynamic and controlled functionality from both the cytoskeleton, the protein networks supporting the cell body, and the cell adhesion machinery, which is connecting the cells to each other and to the ECM. [Conway and Jacquemet, 2019]

Cells have different migration strategies including amoeboid, mesenchymal and lobopodial migration. In amoeboid migration, cells have few weak ECM adhesions, low protease activity, and they push themselves forward using contractile forces or glide on the substrate using actin-driven protrusions. In mesenchymal migration, the cells are strongly attached to the ECM proteins, exhibit high protease activity and they can be described as “crawling” on the surface to move forward. Lobopodial migration represents an intermediate type of migration where tightly adherent cells with low protease activity migrate using actomyosin contractility and hydrostatic pressure with roundish protrusions called lobopodia. Although

specific cell types can favor a certain migration strategy, many of them can switch between these strategies depending on both intracellular regulatory factors and the changing chemical and mechanical properties of their microenvironment, such as ligand specificity and rigidity of the matrix. Furthermore, cells can migrate individually or synchronized in groups referred to as collective cell migration. [Seetharaman and Etienne-Manneville, 2020]

The work presented in this thesis focuses on mesenchymal single cell migration. To understand the basics of mesenchymal single cell migration, the process of cell crawling can be described through a stepwise cycle as presented by an early pioneer of the field, Michael Abercrombie, based on phase contrast and interference reflection microscopy of migrating fibroblast already in the 1970s [Abercrombie, 1970; Abercrombie, 1978]. In this model, first occurs the protrusion of a leading edge, secondly, the adhesions to the ECM, then thirdly cell body contraction and finally, old adhesions are detached at the trailing edge and their proteins are recycled. Although often describe as a stepwise cycle, all these events may overlap and occur simultaneously [SenGupta et al., 2021].

Mesenchymal cell migration is a relevant migration mode for many cell types on traditional 2D cell cultures. Moreover, based on observations on 3-dimensional (3D) collagen gels, organotypic brain slice cultures, and in vivo mouse models, it has been established that glioblastoma cells specifically migrate individually with a mesenchymal mode of motility also in 3D [Zhong et al., 2010]. Moreover, it is a relevant migration mode for studying the impact of ECM proteins for cell polarization and migration, since in mesenchymal migration ECM protein binding through integrin-mediated adhesions play a key role.

1.1.2 Cell cytoskeleton and cell polarization

A dynamic and adaptable cell cytoskeleton, the protein network supporting the cell body, is essential for the cell in maintaining its shape and resisting pressure and tensile forces. It is also fundamental for generating contractile forces to enable cell migration. The cytoskeleton of a mammalian cell is composed of three major types of protein filament networks known as microtubules (MTs), intermediate filaments (IFs) and actin microfilaments. These three protein networks all have different kinds of structural properties and functions, but they work smoothly together to allow cell migration. [Seetharaman and Etienne-Manneville, 2020]

Microtubules are long hollow tube-like structures, composed of α- and β-tubulin and emerge from a microtubule organizing center (MTOC), generally a centrosome. Microtubules are

crucial for transportation of proteins inside the cell, controlling cell shape and position of organelles, as well as associated with cell polarization and focal adhesions. [Hohmann and Dehghani, 2019; Seetharaman et al., 2022] Centrosome positioning and microtubule organization depends on the anisotropy of the actomyosin network and must also be coupled to intermediate filaments. During mesenchymal cell migration, the centrosome, which serves as a MTOC, and the Golgi apparatus are characteristically arranged in front of the cell nucleus, promoting microtubule growth towards the cell front and delivering membranes and associated proteins to form forward protrusions. [Martin et al., 2018]

Intermediate filaments are best known for their ability to provide mechanical strength for the cell. They also influence both cell-ECM adhesion and migration as a signaling platform and mechanically transducing forces through the cell body. [Hohmann and Dehghani, 2019; Seetharaman and Etienne-Manneville, 2020] Whereas tubulin and actin have been strongly conserved in evolution, the family of intermediate filaments is composed of various proteins with a highly cell type specific expression pattern [Hesse et al., 2001].

Polymeric filamentous actin forms double helical structures called F-actin, whereas monomeric globular actin is called G-actin [Rotty and Bear, 2015]. Furthermore, actin is organized to form different kinds of cell structures including flat lamellipodia at the cell front, fingerlike filopodia, contractile stress fibers linked to cell adhesions and contractile actin cortex at the cell membrane. Actin gives the cell its shape, and together with accessory motor proteins, such as myosin II, generates forces responsible of contractions of the cell body during cell migration. [Hohmann and Dehghani, 2019; Seetharaman and Etienne-Manneville, 2020] Monomeric G-actin is polarized, and hence polymeric F-actin, as well as the whole cell cytoskeleton, is polarized as well. The more reactive side of F-actin is termed the (+)-end, and it has a ten times higher polymerization rate than the less reactive side, which is termed the (−)-end. [Pollard, 2016]

The assembly and disassembly of subunits of microtubules, intermediate filaments and actin filaments constantly remodels the cytoskeletal network. Cytoskeleton can react to external and internal signals on the time scale of minutes with a quick assembly and disassembly of protein subunits of these structures. [Hohmann and Dehghani, 2019] Especially the coordinated assembly and disassembly of actin filaments is seen as a driving force for directed movement in mesenchymal cell migration. Important regulators of the organization of actin filaments, and thus cell migration, include e.g. the small GTPases, Rho, Rac, and

Cdc42. [Nobes and Hall, 1999] While the cytoskeleton is assembled and disassembled, new cell adhesions are formed at the cell's leading edge and old adhesions at the cell rear are dissolved, which also requires front-rear polarization, clear structural distinction between the cell's front and rear, with asymmetric distribution of migration related proteins, such as chemosensory signaling receptors, integrins and cytoskeleton linkages [Lauffenburger and Horwitz, 1996; Seetharaman and Etienne-Manneville, 2020].

1.2 Migrating cells interact with surrounding ECM through integrin mediated adhesions

1.2.1 Integrins link the cell cytoskeleton to the ECM

Cell migration takes place in various types of tissues, structures composed of cells and ECM. Some tissues, such as muscle tissue, consist mainly of the cells, whereas some tissues, like fibrous connective tissue, contain only few cells and are mainly composed of the ECM produced by the cells. Each tissue type has its typical composition of water, proteins, and polysaccharides, giving them their characteristic physical properties. Importantly, ECM is not a static structure but dynamically remodeled by the cells, influencing cell proliferation, survival, shape and differentiation. [Daley et al., 2008; Frantz et al., 2010] Cells can pull the ECM through their adhesions, or they can secrete proteolytic enzymes to degrade the ECM and promote cell migration. Conversely, chemical and mechanical properties of the ECM, such as growth factors and cytokines or rigidity and topology of the ECM, can guide cell migration [Alberts et al., 2008; Seetharaman and Etienne-Manneville, 2020].

Integrins, a family of heterodimeric trans-membrane receptors, are the principal cell surface adhesion receptors. The name "integrin" originates from their function of integrating the cell cytoskeleton to the ECM. Accordingly, integrins bind ECM proteins as their primary ligands, coupling the F-actin cytoskeleton to the ECM, and mediating bidirectionally (inside-out and outside-in) cell–matrix (and cell–cell) interactions. [Chastney et al., 2021]

In humans, there are known 18 distinct α and 8 β integrin subunits, which give rise to 24 non-covalently paired αβ-heterodimers. The β1 subunit is the most abundant integrin subunit and it can form heterodimeric complexes with 12 out of the 18 α-subunits. While some integrin subunits or integrin heterodimers are ubiquitously expressed by different types of cells all around the human body, such as the β1 subunit, others are present only in certain tissues or cell types, e.g., β6 subunit is normally expressed in the adults only during wound healing,

αIIbβ3 integrin heterodimer in platelets and α4β7 in specific memory T cells. [Pang et al., 2023; Takada et al., 2007]

Integrin heterodimers have specific affinity to one or more ECM proteins, such as proteins containing Arg–Gly–Asp (RGD) amino acid sequence, including fibronectin and vitronectin, collagen (monomers of fibrillar collagens I, II, III and V via a GFOGER motif in the collagen triple helix) or laminin. Therefore, integrins can be broadly classified into RGD-, collagen-, laminin- and leukocyte-specific types based on their preferred ligands. Besides their main ligands, ECM proteins, integrins also act as cell surface receptors for many non-ECM ligands including growth factors, hormones (e.g., thyroid hormones), and polyphenols. In addition, they are exploited by snake venoms, infectious bacteria (e.g., Borrelia burgdorferi, Yersinia, Helicobacter pylori), viruses (e.g., Cytomegalovirus, Epstein-Barr virus, HIV, SARS-CoV-2), fungal cells and, of course, pharmaceuticals. [Gressett et al., 2022; Huhtala et al., 2005; LaFoya et al., 2018; Pang et al., 2023]

1.2.1 Cell lines and integrin ligands of interest

A glioblastoma (GBM, IDH wildtype) cell line U-251 MG and a breast cancer cell line MDA-MB-231 were used in the micropatterning experiments of this thesis. Both cell lines are adherent, fast-growing, mesenchymal and highly migratory. Directed migration and its regulation is an especially interesting topic in gliomas, since gliomas are typically highly efficient in infiltrating healthy brain tissue, making their complete removal by surgery impossible. Despite advances in treatment, median survival time of glioblastoma patients is only approximately 15 months. [Erices et al., 2023; Koshy et al., 2012; Tran and Rosenthal, 2010] Hence, targeting migratory machinery in gliomas can be a promising approach for the containment of the disease.

Still, a deeper understanding of factors regulating and affecting cell migration behavior is needed for successful targeting and prevention of glioma and other cancer cell migration and metastasis. Better understanding of how cell front-rear polarization directs cell migration, and how ECM binding and integrin signaling modulate migration behavior, can explain why some already existing medical therapies have failed to reach their goals, and enable targeting these processes with new pharmaceutical strategies.

Glioma cells infiltrate the soft brain tissue (composed primarily of hyaluronic acid bound to proteoglycans) preferentially by following more rigid adhesive tracks e.g. myelinated axon

fibers and vascular basement membranes, which consists of various integrin ligands such as fibronectin, collagen and laminin. [Ellert-Miklaszewska et al., 2020] In glioma, upregulation of these proteins is correlated with invasive behavior [Seker-Polat et al., 2022]. Also, in breast cancer, ECM composition and structure undergoes significant changes, and many ECM proteins are upregulated including the fibronectin, fibrillar collagens, and specific laminins [Insua-Rodríguez and Oskarsson, 2016].

The experiments of this thesis investigated fibronectin, collagen I, laminin, and vitronectin, which are integrin ligands, basic components of ECM and relevant in physiological and pathological environments of both glioblastoma and breast cancer.

In addition, two well-characterized monoclonal allosteric anti-human integrin β1 antibodies were used: mAb13 (rat) and 12G10 (mouse). Anti-integrin antibodies are a widely used tool to study integrins, and there are many suitable antibodies for this purpose. The antibodies used in this study, mAb13 and 12G10, both bind to the extracellular domain of the beta-subunit but stabilize different integrin conformations. The mAb13 stabilizes inactive integrin conformation and as such functions as an inhibitory antibody perturbing integrin ligand binding, whereas the 12G10 is a stimulatory antibody, supporting the active form of integrin and enhancing ligand binding. [Byron et al., 2009; Humphries et al., 2005; Mould et al., 1995]

1.2.2 Integrin-mediated adhesion and integrin signaling

Integrin ligand binding on cell membrane is regulated by receptor diffusion within the plasma membrane, intracellular transport of integrins to the binding site and conformational changes of the integrin receptors, which modulate their activity [Conway and Jacquemet, 2019; Humphries et al., 2003]. Generally, bent integrins have low affinity for ligand binding and therefore are considered to be in an inactive state, whereas extended integrins have high affinity for ligand binding, and are considered to be in an active state (Figure 1) [Kanchanawong and Calderwood, 2023; Li et al., 2024; Michael and Parsons, 2020].

Integrin activation and ECM binding initiates recruitment of different intra-cellular proteins leading to formation of adhesions. While extracellular domains of integrins adhere to ligands and thus sense chemical and mechanical properties of their microenvironment, the cytoplasmic domains (tails) of integrins can trigger intracellular signaling resulting in integrin clustering and the assembly of heterogenous multiprotein structures, termed as integrin adhesion complexes (IACs).

Key components of these complexes include integrins and cytoplasmic proteins such as kindlin, talin, paxillin, focal adhesion kinase (FAK) and Src, which create binding sites for other structural and signaling proteins, and link integrins e.g., to phosphoinositide- 3-kinase (PI3K)/AKT pathway, the rat sarcoma virus (RAS) proteins or small GTPases (Rac1 GTPases) -mitogen-activated protein kinase (MAPK) pathways enabling sophisticated tuning of cell survival, proliferation, polarization and migration through cytoskeletal changes and activation of gene transcription. These signaling pathways are also relevant to cancer initiation, progression, metastasis, angiogenesis, and inflammation. [Alday-Parejo et al., 2019; Bachmann et al., 2019; Ellert-Miklaszewska et al., 2020]

These cell-ECM adhesion and signaling platforms can be divided into different subtypes based on their morphological features and protein composition, including classical IACs such as nascent adhesions, focal complexes, focal adhesions (FAs), filopodial adhesions and fibrillar adhesions. Additionally, integrins are involved in specialized atypical IACs including clathrin plaques, hemidesmosomes, podosomes, invadopodia and immunological synapses. [Chastney et al., 2021; Conway and Jacquemet, 2019]

1.2.3 Integrin-targeting therapies

Integrin structure and binding is highly conserved during the evolution of vertebrates. [Takada et al., 2007]. Abnormalities in integrin activity are associated with disturbed cell adhesion and migration behavior and are linked to several diseases, including chronic inflammation and cancer. Integrins are one of the major targets to affect cell migration with pharmaceuticals. In addition, many drugs modify ECM, and thus the compositions of integrin ligands, to a more beneficial direction as a by-product of their primary mechanism of action. It is also recognized that directly targeting the ECM could significantly advance the treatment of various diseases with unmet medical needs. [Järveläinen et al., 2009]

Integrins have been investigated as pharmacological targets for nearly 40 years and still are actively targeted in preclinical studies and clinical trials by new drug candidates. Still, to date, there are surprisingly few integrin targeting drugs on the market approved by the U.S. Food and Drug Administration (FDA): abciximab (ReoPro), natalizumab (Tysabri and its biosimilar Tyruko), vedolizumab (Entyvio), eptifibatide (Integrilin), tirofiban (Aggrastat) and lifitegrast (Xiidra). In addition, excitingly, in March 2022, was approved in Japan the first oral anti-integrin drug, carotegrast methyl (Carogra), used for treatment of ulcerative colitis. Whereas natalizumab, vedolizumab and abciximab are biological drugs, eptifibatide,

tirofiban, lifitegrast and carotegrast methyl are small molecules. [Dhillon, 2022; Pang et al., 2023; Shirley, 2024; Slack et al., 2022]

Abciximab (ReoPro), an αIIbβ3 antagonist, was approved by the FDA in 1994 to treat clotting disorders, and it was the first anti-integrin therapeutic in clinical use. [Bachmann et al., 2019]. Whereas, probably best-known of the approved anti-integrin drugs are Biogen's top-selling drug natalizumab (Tysabri) used for multiple sclerosis and Crohn's disease, and Takeda's vedolizumab (Entyvio) used for ulcerative colitis and Crohn's disease.

Efalizumab (Raptiva), an anti-integrin therapy was approved by the FDA to treat psoriasis in 2003, but withdrawn from the market in 2009, after it was linked to increased risk of a rare, but often-fatal, brain infection called progressive multifocal leukoencephalopathy (PML), which is caused by a general opportunist virus called John Cunningham virus (JCV) when leukocyte trafficking to the central nervous system is reduced due to drug inhibition. For the same reason, natalizumab, which was approved in 2004, carries a black box warning. Interestingly, vedolizumab has not been shown to increase the risk for PML, which is believed to be due to its specificity against α4β7-heterodimer. [Cully, 2020; Pang et al., 2023]

Integrin-targeting anti-cancer therapies, despite convincing preclinical data and encouraging preliminary results, have unfortunately not met the expectations in clinical trials. Especially the discontinuation of cilengitide, an inhibitor of αvβ3 and αvβ5 integrin receptors, after phase III trial for treatment of glioblastomas was a major disappointment for integrin-focused drug development. Deeper understanding of integrin structures, function and complexity in health and disease is still needed. [Conway and Jacquemet, 2019]

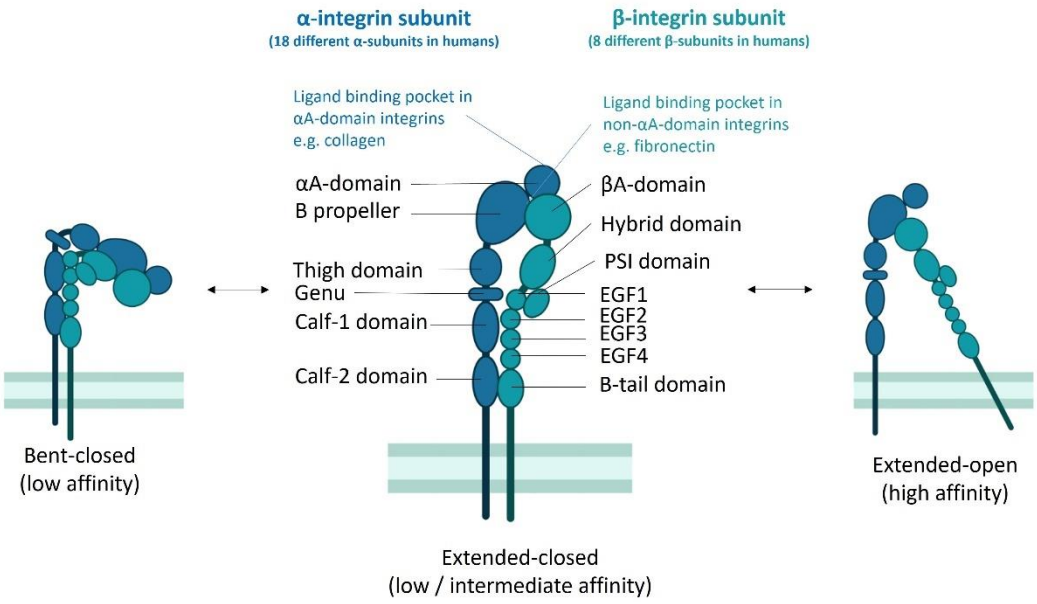

Figure 1. Integrins are heterodimeric transmembrane receptors composed of α- and β-subunits. They mediate inside-out and outside-in cell-matrix (and cell-cell) signaling and have an important role in cell polarization, adhesion and migration. Conformational changes modulate integrins' ligand binding affinity. Integrin structure is presented here based on Humphries et al. 2003. Figure created in Biorender.com.

1.3 Geometric control of cell polarization and migration

Various chemical and mechanical properties of the ECM can trigger and modulate cell migration behavior. These include chemical cues such as growth factors and cytokines, as well as mechanical properties of the cell microenvironment such as the rigidity and topology of the ECM. Unequal distribution of these signals forming gradients can direct and guide cell polarization and migration e.g., towards a chemoattractant, from softer substrate to a more rigid area, or the other way around. In addition, intracellular factors can direct cell migration by creating migration promoting gradients e.g., by pulling the ECM using integrin-based adhesions, or by degrading the ECM proteins with proteases. [Sarkar et al., 2020; Seetharaman and Etienne-Manneville, 2020] Also, geometry of cells' microenvironment, and more specifically, the geometry of cells' adhesive microenvironment, is known to influence cell polarization and the direction of cell migration. [Jiang et al., 2005; Segerer et al., 2016; Théry et al., 2006]

Jiang et al. (2005) described that confining 3T3 fibroblasts, COS-7 fibroblasts, and human umbilical artery endothelial cells (HUAC) to asymmetric micropatterns, including teardrop-shapes and triangles, forced the cells to polarize and consequently, when the 3T3 fibroblast were electrochemically released from their confined shapes, guided their direction of

movement. Furthermore, they concluded that cell polarity itself, characterized by a wide spreading front and a narrow rear, can determine the cell's direction of motility. [Jiang et al., 2005] Soon after, Thery et al. (2006) published their findings on how asymmetrical fibronectin-coated micropatterns directed the internal and cortical orientation of human retinal pigment epithelial (RPE) cells. They noticed that crossbow-shaped micropatterns created an adhesive leading edge, which supported polymerizing actin meshwork within membrane ruffles, and non-adhesive sides, which supported the formation of contractile actin stress fibers [Théry et al., 2006]. In Figure 2, I present, based on findings of Thery et al., a schematic illustration of characteristic features of a polarized cell moving via mesenchymal migration (Figure 2. A) and a polarized cell confined to a crossbow-shaped micropattern. (Figure 2. B).

Different shapes of adhesive micropatterns have shown different levels of control over cell polarity [Jiang et al., 2005; Théry et al., 2006]. However, the impact of different adhesive substrates (matrix proteins or anti-integrin antibodies), for controlling front-rear polarization and migration is still not known.

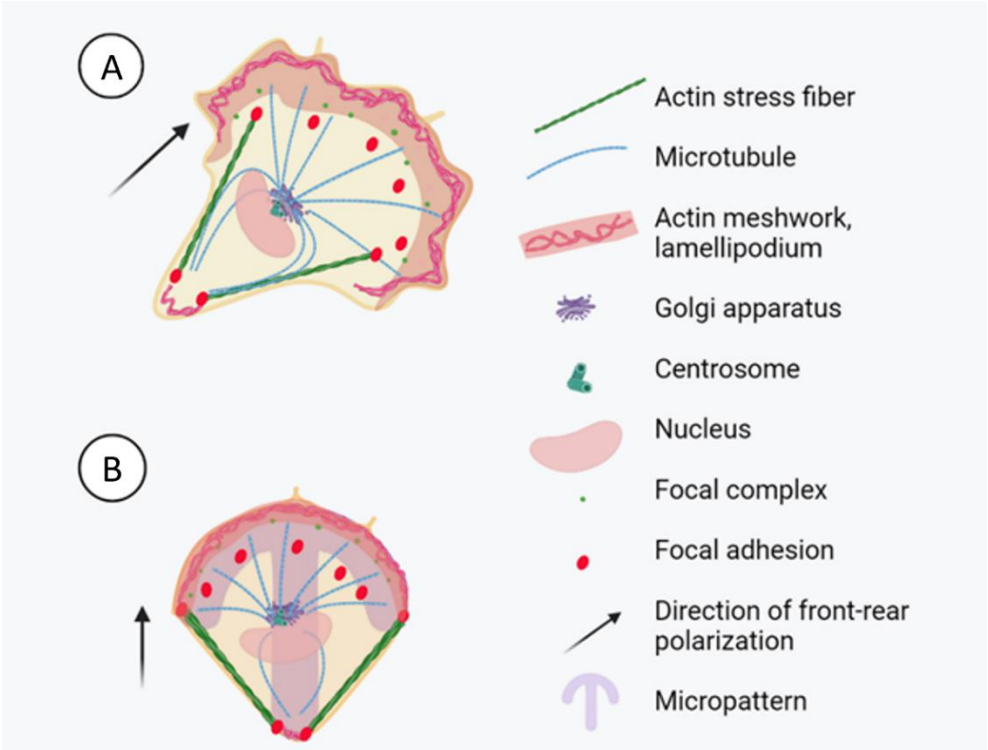

Figure 2. A) In mesenchymal cell migration, Golgi apparatus and centrosome are typically localized in front of the nucleus. B) Asymmetric single-cell micropatterns, such as crossbow-shaped micropatterns, can guide cells to polarize and form a leading edge towards the wider and more adhesive side of the micropattern. [Théry et al., 2006] Figure created in Biorender.com.

1.4 Protein and cell micropatterning in biomedical sciences

1.4.1 Micropatterning and its applications in biomedical sciences

The term micropatterning describes a variety of techniques to precisely control the distribution of surface molecules, with micrometer resolution [Watson et al., 2021], including controlling the placement and microenvironment of living cells on a culture surface. In research, making general observations of cell populations often requires focusing on changes and behavior of certain individual cells. In 1967, Carter described a method to produce small adhesive island (150 x 100 µm) to observe simultaneously a large amount of single cells over long time-periods, and presented the idea and many benefits of cell micropatterning [Carter, 1967]. To this day, the benefits of micropatterning have been widely acknowledged, and protein and cell micropatterning have become important tools to study fundamental cell biology. Cell micropatterning can be used to precisely control the shape, orientation and number of cell-cell and cell-ECM interactions of single cells, and then utilized to investigate how the physical microenvironment and surface chemistry regulate cell differentiation, adhesion, spreading, and eventually, cell fate. [Nakanishi et al., 2008; Théry, 2010]

The control of cell adhesion geometry reduces the variability of the cells, in and between experiments, which can improve the accuracy, sensitivity and quality of the visualization and quantification of drug effects or differences between the study groups. This helps detect statistically significant differences between the groups of interest with fewer cells and smaller amounts of expensive investigational medicines or other materials. [Degot et al., 2010; You and Piehler, 2016]

Furthermore, different protein and cell micropatterning methods have enabled the development of a wide range of applications such as tissue engineering, cell-based drug screening and cell-based sensors. Tissue engineering, designing and building cellular microenvironments to mimic living tissues and organs (e.g., hepatocyte spheroids), is important for finding *in vitro* models for drug screening purposes, ideally even as alternatives for animal experiments, but also for developing new transplantation applications. Micropatterning has also been used to improve sensitivity to identify drugs and toxins in methods measuring active potentials of electrically active cells, including neurons and cardiac cells. Cell microarrays, micropatterned chips used to detect the expression of thousands of genes at the same time, are an example of cell-based sensors, and expected to be new

platforms for more sensitive high-content and high-throughput drug screening. [Nakanishi et al., 2008; Salomaa, 2020; Yap and Zhang, 2007]

1.4.1 Protein and cell micropatterning techniques

The most common strategy for producing micropatterns for cell culture is to create a chemically patterned surface with adhesive and non-adhesive areas. Several methods have been described for controlling cell attachment with proteins, which promote cell adhesion, such as fibronectin, laminin, and collagen, used in combinations with areas of inert, non-adhesive materials.

Typically, chemically patterned surfaces are produced via soft lithography or photolithography. Soft-lithographic methods include two major techniques for surface patterning: microcontact printing and microfluidic patterning. In microcontact printing, the patterning material is transferred to the surface using a stamp. In microfluidic patterning, a stamp is used to create a network for microfluidic injections of the patterning material solution. In photolithography, the desired micropatterns are created to a photoactive surface with a laser device or by exposing it to UV irradiation through a photomask. Photomasks of different designs can be easily purchased from commercial suppliers and used as many times as needed. Compared to stamping, photolithography combined to protein coating by incubation allows to vary the concentration of protein attached to the surface, either by adjusting the concentration of the protein solution or the time of incubation. However, usually photolithography requires a more dust-free working environment than soft lithography. [Segerer et al., 2016]

With both soft-lithography and photolithography, the development of synthetic anti-fouling materials has been a key step in successfully controlling cell adhesions on micropatterns. One of the most commonly used anti-fouling materials is poly(l-lysine)-graft-poly(ethylene glycol) (PLL-g-PEG), which is a random graft co-polymer with a poly(L-lysine) backbone and poly(ethylene glycol) side-chains. [Nakanishi et al., 2008]. Poly-L-Lysine (PLL) is a positively charged synthetic amino acid, which binds to the negatively charged glass surface anchoring the PEG to form a highly hydrophobic and non-adhesive surface. [Elbert and Hubbell, 1998]

In addition to chemically patterned surfaces, other patterning strategies include, for example, seeding cells on a topographically patterned surface, or direct delivery of cells onto discrete

regions of a substrate. In commercial use, robotic spotters can be used for faster production of highly complex surface patterning with biomolecules. [Nakanishi et al., 2008; Yap and Zhang, 2007]

When choosing an appropriate micropatterning method, one should consider if it is aimed for single-cell micropatterning or patterning of cell sheets or networks. Microfluidic patterning is not suitable for single-cell micropatterning, and neither are all stamps and photomasks. Also, access to clean room might be needed for more ambitious micropatterning goals. Often the available resources and costs determine which methods can be considered for each experiment, and compromises are needed to minimize the need for specialized equipment, but still maintaining the good micropatterning quality.

1.4.2 Dynamic micropatterning

Modifiable, dynamic micropatterns enable the alteration of cell adhesiveness of the micropatterned areas at any chosen time-point (Figure 3.). The possibility to selectively modify micropatterns during or after cell attachment has opened new possibilities in life sciences. Techniques to create modifiable, dynamic, micropatterns have included altering the cell or protein adhesiveness of the surface with UV exposure, electrochemical stimulation or addition of linkable ligands [D'Arcangelo and McGuigan, 2015; Nakanishi et al., 2008]. For such applications, it is important to be able to change the cell or protein adhesiveness with no cytotoxic effect on living cells, which can sometimes be challenging.

Micropatterns provide an opportunity to study single isolated cells in standardized microenvironments. With dynamic micropatterning the attached cells can be released to migrate and create ligand-receptor interactions in a more controlled and standardized manner than in traditional cell culture. This feature can be utilized in co-culturing multiple cell types and analyzing dynamic cellular activities, like cell polarization and migration. One of the best-known traditional methods to study polarized, moving cells is to scratch a line in a confluent monolayer of cells to observe how they spread from the edges of the empty space to fill the "wound". Micropatterns, in contrast, provide an opportunity to study single isolated cells and control their microenvironment's e.g., shape and ECM composition, without the complications of varying amount of cell–cell contacts.

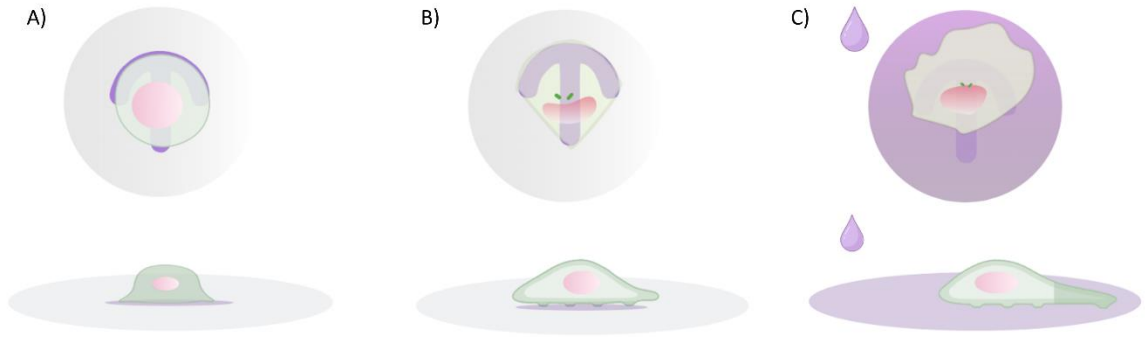

Figure 3. The concept of dynamic single-cell micropatterning. Figure created in Biorender.com.

A) Cells settle and adhere to the adhesive protein coated micropatterns.

B) Cells spread on the micropatterns and adopt the pattern shape. Asymmetric micropatterns can direct the cell front-rear polarization, depending on cell adhesive environment and cell type [Jiang et al., 2005; Théry et al., 2006].

C) Dynamic micropatterning with linkable ligands enables the alteration of cell adhesiveness around the protein-coated micropatterns just by adding a few drops of medium containing streptavidin-conjugated adhesive proteins. Streptavidin rapidly binds to the biotin of the inert surface, tethering the adhesive proteins (e.g. fibronectin) and making the surface accessible for cell migration. Thus, micropatterned cells can be released to create new ligand-receptor interactions and migrate from their confined shape in a controlled and standardized manner.

1.5 Aims of the project

In this project, I tested a method utilizing biotin – streptavidin binding to produce dynamic micropatterns for single-cell studies. Compared to more traditional micropatterning with adhesive patterns and non-adhesive background, dynamic micropatterning allows transforming the non-adhesive areas surrounding the cells into adhesive at any chosen time point, therefore releasing the cells to migrate.

The method to produce dynamic micropatterns was developed and optimized based on a protocol by Azioune et al. (2009) for generating static micropatterns and had already partly been adapted to the laboratory where I carried out this work. The original method had been modified by using biotinylated PLL-g-PEG instead of conventional (unconjugated) PLL-g-PEG and applying streptavidin-conjugated matrix proteins in the culture medium. The method for dynamic micropatterning could be broken into the following steps: 1) Surface preparation and coating with biotinylated PLL-g-PEG, 2) Micropatterning using photolithography (UV light exposure), 3) Protein coating of UV-exposed micropatterns, 4) Seeding the cells on the micropatterns, 5) Releasing the cells to migrate by adding streptavidin-conjugated matrix

proteins to the culture medium. (Figure 4.). Streptavidin forms a strong bond with the biotin in PLL-g-PEG-biotin layer (between the micropatterns), even in complex protein mixtures, while the PLL-g-PEG itself will still prevent nonspecific adsorption of other proteins.

This thesis project was a part of validating the presented dynamic micropatterning method by demonstrating that the technique works as desired. Verifying that the research method is robust, reliable and reproducible increases the value of later experiments by ensuring that the obtained results can be trusted. Therefore, a set of laboratory tests was performed to investigate the quality of the method. After method validation, the method for dynamic micropatterning was applied for studying the impacts of different ECM compositions (integrin ligands) on cell front-rear polarity and subsequent directed migration.

The project covered three specific aims:

1) To investigate the coating efficiency and specificity of streptavidin-conjugated integrin ligands to PLL-g-PEG-biotin-coated surfaces.

2) To investigate the biocompatibility of PLL-g-PEG-biotin surfaces for single-cell micropatterning.

3) To investigate the role of different ECM components and anti-integrin antibodies in supporting front-rear polarization and directed single-cell migration.

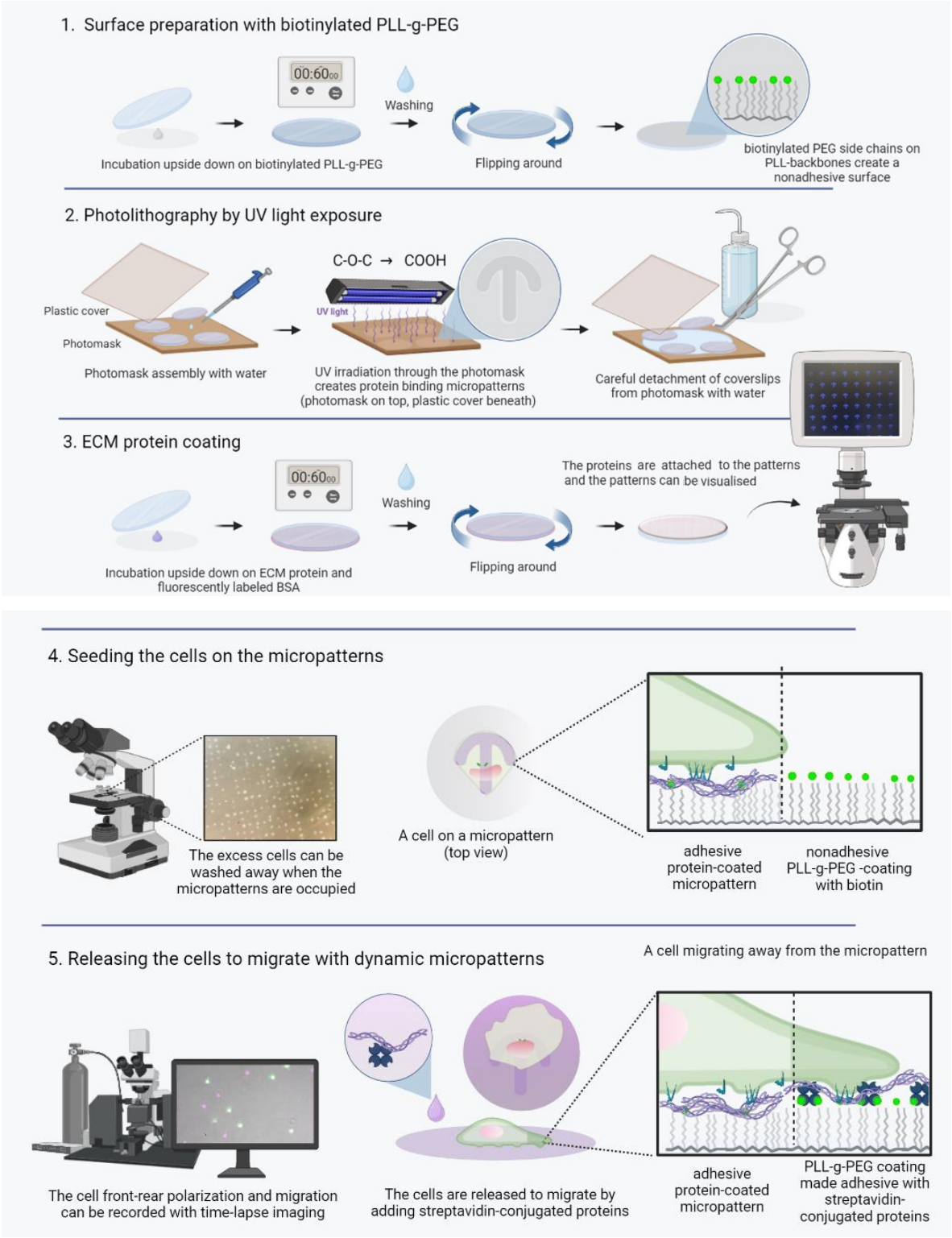

Figure 4. The process of visualizing and controlling cell polarization, adhesion, and migration using biotinylation-based dynamic micropatterning. 1) Biotinylated PLL-g-PEG is used to create a nonadhesive surface. 2) UV exposure through a photomask modulates the surface creating protein binding micropatterns. 3) The micropatterns can then be coated with protein of choice. 4) Cells attach to the adhesive protein coated micropatterns adapting their shape, but not to the surrounding PLL-g-PEG. 5) The cells can be released to migrate from their confined shape by adding streptavidin-conjugated adhesive proteins, which rapidly bind to the biotin of the biotinylated PLL-g-PEG. Figure created in Biorender.com.

2 Results

2.1 Coating efficiency and specificity of streptavidin-conjugated integrin ligands to PLL-g-PEG-biotin-coated surfaces

The first concrete aim of the project was to investigate the coating efficiency and specificity of streptavidin-conjugated integrin ligands to PLL-g-PEG-biotin-coated surfaces. Therefore, the first action was to prepare a series of micropatterned cover glasses with different concentrations of streptavidin-conjugated ligands to show whether the amount of ligand on the biotinylated surface can be controlled in a linear manner. Next, we sought to investigate the specificity of the streptavidin-biotin bond in controlling ECM protein placement on and off the photopatterned regions.

2.1.1 Coating density of streptavidin-conjugated ligands on biotinylated PLL-g-PEG can be altered by using different ligand concentrations

Experiments with different concentrations of streptavidin-conjugated fibronectin (0, 1, 5 or 15 µg/ml) were performed to inspect the coating efficiency of biotinylated PLL-g-PEG, and to assess whether the amount of secondary ligand on the surface between the UV-exposed micropatterns can be controlled in a linear manner (Figure 5. A). Of each micropatterned and protein-coated cover glass, multiple regions were imaged with immunofluorescence microscopy to create a representative overall picture of each glass.

Although the general quality of the patterns was good, there was some variation inside each glass coverslip between different fields of views. Typically, the center of each glass coverslip was the best-looking area and the patterns were weaker on the edges of each glass. Also, some small ”bubbles” were present in the coating, appearing as full of either red (BSA-AF555) or green (anti-fibronectin 488) in the immunofluorescence imaging. Obviously unsuccessful areas with poor patterning were excluded.

The variation between signal intensities of the measured areas in each field of view was minimal, even though the imaging technology was anticipated to lead to slightly stronger signal in the middle of each image than on the edges (i.e., vignetting). The streptavidin-conjugated ligand, fibronectin, bound to the biotin in the areas surrounding the blocked micropatterns, as expected. The protein density on the surface increased with more concentrated working solutions, although it seemed that the surface got saturated already with

the fibronectin working solution of 15 µg / ml. (Figure 5. B). Therefore, different protein concentrations can be used to manufacture surfaces with different coating densities.

Encouragingly, the amount of fibronectin on the actual micropatterns did not seem to increase considerably (Figure 5. C), indicating that the BSA blocking was enough to prevent non-specific binding and implying that the biotin might be detached or inactivated during the UV-exposure as described before by Biswas et al. [Biswas et al., 2013]. These findings suggest that the new technique for dynamic micropatterning is suitable for producing binary micropatterns with two distinct protein surfaces and is therefore a viable tool for studying cell behavior at the interface of different ECM protein conditions.

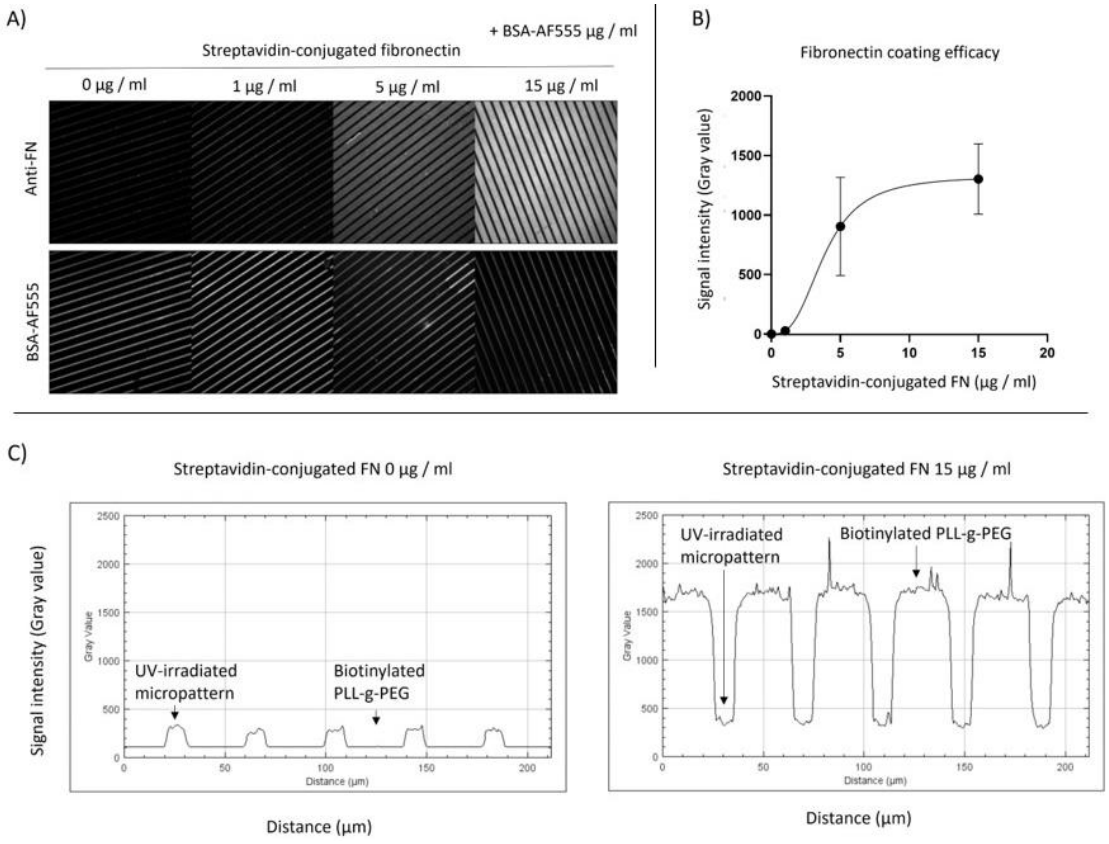

Figure 5. Coating efficiency of streptavidin-conjugated fibronectin was investigated with four different concentrations (0,1,5 and 15 µg / ml). A) Fibronectin was visualized with immunofluorescence staining and Alexa Fluor 555-labelled BSA was used to visualize UV-exposed stripes and to ensure patterning quality. The streptavidin conjugated fibronectin bound to the biotin between the micropatterned stripes (9 µm wide stripes), and higher concentrations of streptavidin-conjugated fibronectin in the protein coating solution led to higher density of streptavidin-conjugated fibronectin on the coated surface. B) Fibronectin coating efficacy presented as mean and standard deviation (SD). The average background signal was subtracted from the measured signal intensities, and Specific binding with Hill slope -equitation was used to fit the curve. The efficacy of streptavidin-conjugated fibronectin coating was studied with four different coating concentrations (0,1,5 and 15 µg / ml) and the number of imaged field of views in each condition was 8, 7, 7 and 6, accordingly. The mean signal intensities from fibronectin stripes in each field of view was obtained by measuring ten separate areas of each imaged view with Image J. C) Example intensity profiles of fibronectin signal on surfaces coated with 0 µg / ml

and 15 µg / ml of fibronectin. Variation between the measured areas inside each field of view was minimal.

2.1.2 Streptavidin-conjugated ligands enable producing binary micropatterns with areas of two distinct protein compositions

The specificity of the protein coating in cell micropatterning, i.e., the ability to control protein binding and cell attachment either on the photopatterned micropatterns or the uninterrupted biotinylated PLL-g-PEG around them, was further investigated by imaging MDA-MB-231 cell attachment and spreading on binary micropatterns with lines of adhesive and non-adhesive areas.

For this purpose, four kinds of micropatterns were manufactured: UV-exposed stripes coated with either 1) fibronectin or 2) collagen I, with uninterrupted biotinylated PLL-g-PEG coating between them, and 3) uncoated UV-exposed stripes, with added streptavidin-conjugated fibronectin fragment, FNIII (7-10), or 4) uncoated UV-exposed stripes with added streptavidin-conjugated collagen fragment, GFOGER, between them (Table 1.).

The MDA-MB-231 cells were allowed to attach and spread for 3 hours on the micropatterned glass coverslips before they were fixed and stained. Immunofluorescence staining of integrin-mediated adhesions (marked by paxillin) revealed that the adhesions were formed where proteins were added to facilitate cell attachment, according to the coating protocol (Figure 6).

Firstly, the acquired data further confirmed that UV photopatterning of biotinylated PLL-g-PEG and streptavidin-conjugated secondary ligands can be used to produce binary micropatterns with two discrete coating compositions. Secondly, the method can be used to manipulate the localization of IACs, and to observe cell attachment in different, complex environments.

Table 1. Four types of micropatterns were manufactured to study the specificity of the protein coating either on the photopatterned micropatterns or the biotinylated PLL-g-PEG around them.

Condition	UV-irradiated micropatterns on biotinylated PLL-g-PEG	Uninterrupted biotinylated PLL-g-PEG coating
1.	Fibronectin + BSA-AF555	-
2.	Collagen I + BSA-AF555	-
3.	BSA-AF555	Streptavidin-FNIII (7-10)
4.	BSA-AF555	Streptavidin-GFOGER

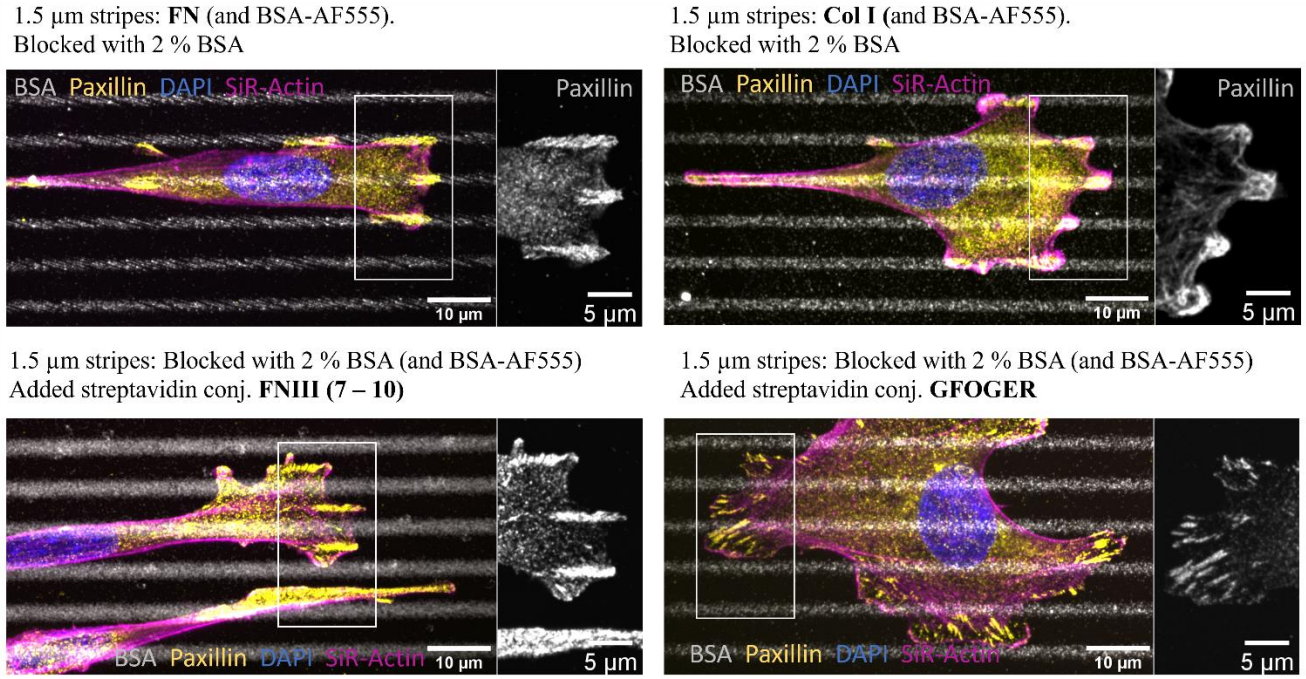

Figure 6. MDA-MB-231 cell adhesion was investigated on UV-exposed micropatterns coated with fibronectin (FN) or collagen I (Col I), and between the UV-exposed micropatterns, where streptavidin-conjugated fibronectin fragment, FNIII (7-10) or streptavidin-conjugated collagen fragment, GFOGER, had been added. The micropatterns were visualized with Alexa Fluor 555-conjugated BSA. The localization of paxillin-positive IACs demonstrates that streptavidin-conjugated ligands enable producing binary micropatterns with areas of two distinct protein compositions.

2.2 Biotinylated PLL-g-PEG is biocompatible for micropatterning purposes

The second concrete aim of the project was to confirm that the biotin of the biotinylated PLL-g-PEG surfaces does not disturb or change the cells' morphology, cytoskeleton arrangement or ability to form adhesions compared to cells seeded on micropatterns on conventional PLL-g-PEG surfaces. When investigating subtle biological functions in cell research, it is important that the experimental conditions or materials are not unintentionally cytotoxic or otherwise manipulate cell behavior by causing unrecognized harm to the cells.

To confirm the suitability of biotinylated PLL-g-PEG for producing micropatterns for cell research, U-251 MG glioblastoma cell morphology on micropatterns prepared on biotinylated PLL-g-PEG was compared to U-251 MG glioblastoma cell morphology on micropatterns prepared on conventional PLL-g-PEG. To observe and compare differences between the two cell groups, the cells were allowed to attach and spread on fibronectin-coated crossbow-shaped micropatterns for 3 hours, then fixed, immunofluorescence stained and imaged. The images were reoriented and aligned based on their micropatterns to overlay the cells of each

group. Thereafter, average intensity projections from actin and paxillin channels of overlaid cells were created both as grayscale projections and heatmaps (Figure 7.).

No visible differences were observed in the average spatial distribution of actin or IACs (visualized by paxillin) when comparing cells on biotinylated PLL-g-PEG to cells on conventional PLL-g-PEG. Therefore, biotinylation of PLL-g-PEG does not obviously alter normal cell morphology on the micropatterned substrates and is biocompatible for the intended use.

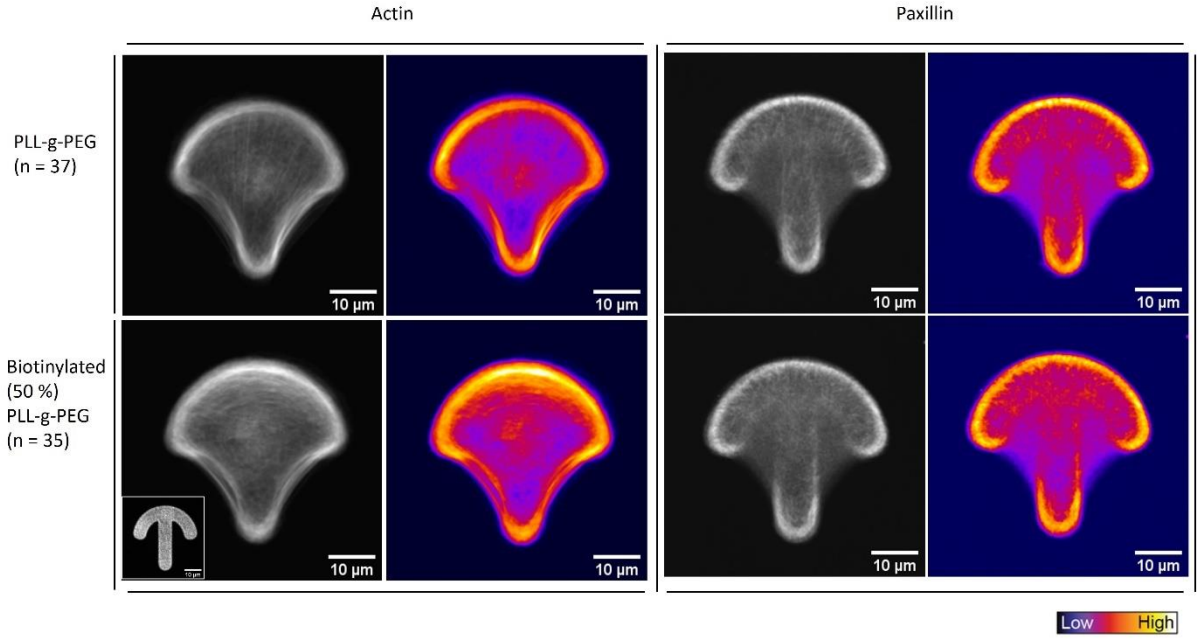

Figure 7. Averages (grayscale) and heatmaps of actin and paxillin distribution in U-251 MG cells seeded on fibronectin-coated micropatterns, manufactured either on PLL-g-PEG (n = 37) or biotinylated (50 %) PLL-g-PEG surface (n = 35). Average actin and paxillin distributions of the imaged cells did not show any differences in cells' actin cytoskeleton or paxillin-positive adhesion sites, indicating that biotinylated PLL-g-PEG is as biocompatible as normal PLL-g-PEG for micropatterning purposes. An example micropattern in inset. All scale bars are 10 µm.

Interestingly, during this experiment, considerably weaker signals were obtained from micropatterns, which were occupied by the U-251 MG cells compared to the empty micropatterns. This suggest that the U-251 MG cells deplete or modify the micropattern coating on the micropatterns rather quickly, already within few hours, which might need to be taken into consideration when planning experimental designs (Figure 8.). One field of view was captured to record this observation, but this phenomenon could be further investigated systematically in the future.

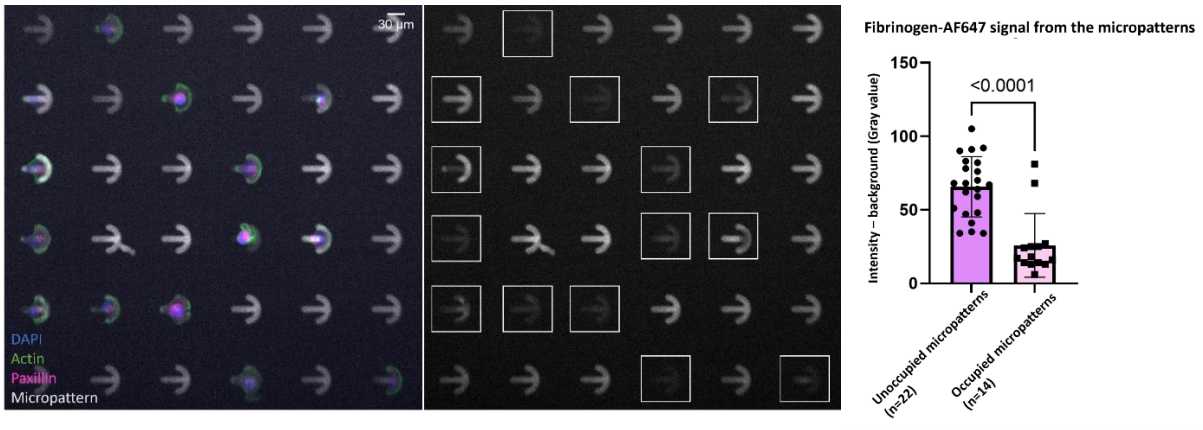

Figure 8. The fibrinogen-AF647 signal from micropatterns occupied by U-251 MG cells were considerably weaker than from unoccupied micropatterns, which suggests that U-251 MG cells may significantly deplete or modify the protein coating of the micropatterns already within a few hours. Here is presented a view with 6x6 crossbow-shaped micropatterns: on left, all imaged channels merged, whereas on right, only the micropatterns shown and occupied micropatterns annotated with white squares. Of these 36 micropatterns, 14 were occupied by U-251 MG cells. The bar chart represents the average signal intensities of each micropattern, their mean and SD. The background signal was subtracted from the measured signal intensities before graphing, and Mann-Whitney test was used to compare the two groups.

2.3 The impact of different ECM components and anti-integrin antibodies on supporting cell front-rear polarization and directed cell migration on dynamic micropatterns

After the technical validation of the new dynamic micropatterning method, the front-rear polarization and its effect on cell migration was investigated in cells cultured with different ECM components (integrin ligands) or in conditions where integrin clustering and activation are manipulated with anti-integrin antibodies. Studying these questions can be applied, for example, to understand and target the crucial steps of cell migration and cancer metastasis.

Although many factors are known to influence how cells adapt their direction of front-rear polarity, there have not yet been any systematic comparisons of cell front-rear polarization on different ECM components, or integrin ligands. Therefore, dynamic micropatterning was applied to investigate front-rear polarization of U-251 MG cells on crossbow-shaped (d = 37 µm) micropatterns and its subsequent effect on cell migration, when cells were cultured on micropatterns with different ECM proteins (integrin ligands) or on anti-integrin antibodies raised against the active (extended-open; clone 12G10) or inactive (bent-closed; clone mAb13) conformations of integrin β1.

Firstly, we investigated whether the direction of front-rear polarization induced by geometric cues is affected by the type of integrin ligand the cells are interacting with. Thereafter, the front-rear polarization of cells on different integrin ligands was tracked using live-imaging. Finally, U-251 MG cells were released to migrate from fibronectin- or mAb13-coated crossbow-shaped micropatterns by adding streptavidin-conjugated fibronectin to the culture medium. Additionally, integrin activation and signaling on different ligands was studied in U-251 MG cells by Western blotting.

2.3.1 Cell front-rear polarization on crossbow-shaped micropatterns varies depending on the integrin ligand used for protein coating

To investigate whether the direction of front-rear polarization induced by geometric cues is affected by the type of integrin ligand the cells are interacting with, crossbow-shaped micropatterns were coated with one protein of interest, including ECM components recognized by integrins: fibronectin, type I collagen, vitronectin, and laminin, as well as anti-integrin β1 antibodies: mAb13 and 12G10. Then, U-251 MG cells were allowed to attach and spread to the protein-coated micropatterns, fixed, immunofluorescence stained and imaged.

As expected, the fibronectin-coated crossbow-shaped micropatterns were highly efficient in controlling the direction of U-251 MG front-rear polarization (Figure 9. A). Accordingly, they were considered as the polarized control and the cells on the other ECM components were compared to the cells on the fibronectin. It was observed that like fibronectin, also laminin (LN-521) highly supported front-rear polarization towards the wider edge of the adhesive micropattern (Figure 9. D). In contrast, cells spread on collagen-coated patterns were significantly less polarized towards the wider edge of the micropattern compared to cells on fibronectin-coated patterns (Figure 9. B). On the vitronectin coating, although previous tests by the lab (data not shown) had suggested otherwise, the U-251 MGs were surprisingly poorly polarized towards the wider edge of the micropattern (Figure 9. C).

With both anti-integrin antibodies cell adhesion and spreading on the patterns was partially disturbed. There were many round cells, and overall, much less cells attached compared to other conditions. Also, there were especially many double-occupied patterns with inhibiting antibodies. Since the cells had difficulties attaching properly on the micropatterns, they may have been more disposed to aggregate together. Nevertheless, when observing single cells that had fully spread to the antibody-coated micropatterns, both antibodies were supporting at least partially front-rear polarization towards the wider edge of the crossbow-shaped

micropatterns (Figure 9., E & F). Interestingly, the cell attachment and polarization seem to be more disturbed with integrin activating 12G10 antibody than with mAb13. However, the data should be interpreted with caution until pooled with at least two other repeats of the experiment.

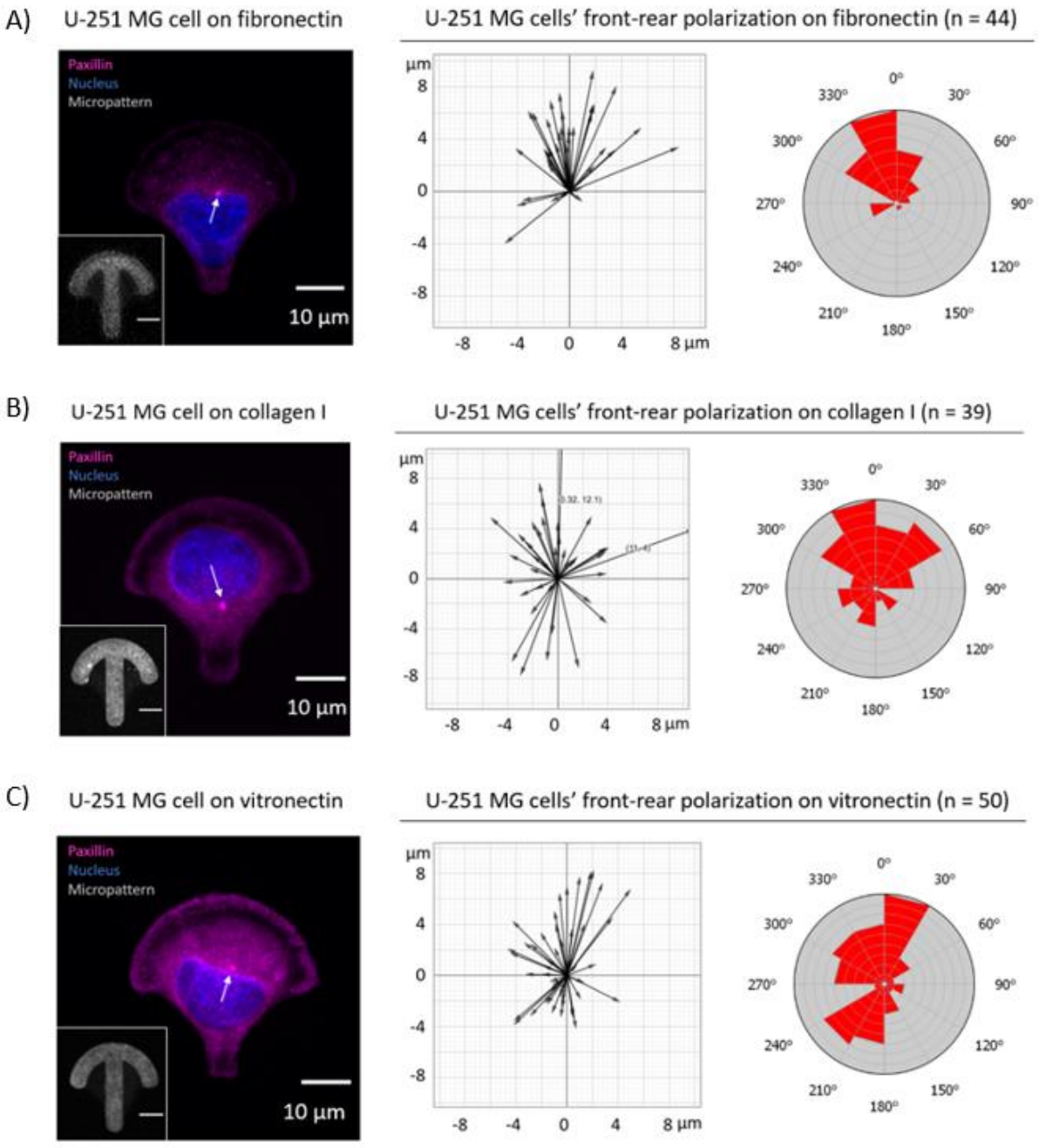

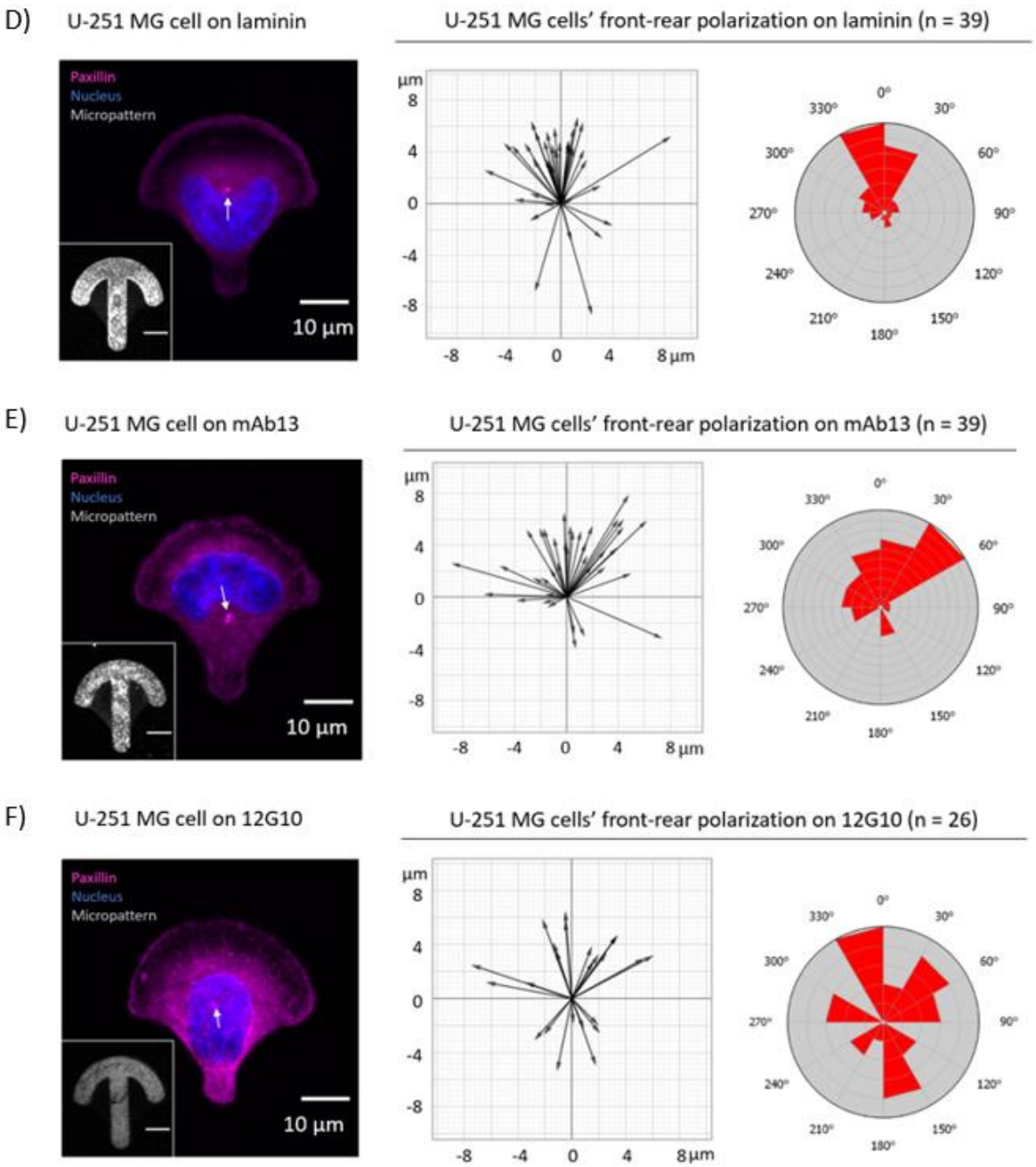

Figure 9. U-251 MG cell polarization on crossbow-shaped micropatterns coated with either A) fibronectin, B) collagen I, C) vitronectin, D) laminin, E) mAb13 or F) 12G10. Cell front-rear polarization, measured as nucleus-centrosome vector, varied depending on the integrin ligand used for protein coating. Of the tested substrates, fibronectin and laminin seemed to be the most effective in controlling U-251 MG cell polarization on crossbow-shaped micropatterns.

On the left, an example cell as a merged image where paxillin is shown with magenta and nucleus with blue. The micropattern under the cell is presented separately (inset). In both images the scale bar is 10 µm. The white arrows annotate the location of the centrosomes in the example cells and indicate an estimation of front-rear polarity of these cells.

In the middle and on the right, the plots describe the direction of front-rear polarization of all imaged U-251 MG cells on each six protein coatings. The direction of the cell polarization was determined as the direction of the centrosome in relation to the cell nucleus, or in other words, the angle of the nucleus – centrosome vector. In the middle, the results are visualized as nucleus – centrosome vectors (presented as the nucleus being the origo).

2.3.2 Live-imaging confirmed that geometric control of front-rear polarization depends on coating composition and cell type

Before moving to the live-imaging of cell polarization and migration with dynamic micropatterns, live-imaging was tested by applying it to study the dynamics of cell front-rear polarization without releasing the cells to migrate. To track the localization of centrosomes in living and moving cells, transfected cell lines stably expressing fluorescent centrin-2 were generated from both the U-251 MG cells and MDA-MB-231 cells. Cell sorting was used to increase the percentage of successfully transfected cells and to obtain cell populations with more even expression levels of the green fluorescent protein. With both cell lines, the transfection was successful and the transfected cell lines viable.

The front-rear polarization of U-251 MGs on crossbow-shaped micropatterns was then studied by imaging live cells on fibronectin- and mAb13-coated micropatterns. Based on the data of the front-rear polarization of fixed cells (data above, Figure 9.) and previous experiments by the lab (data not shown), the majority of the U-251 MG cells were expected to polarize towards the wider edge of the crossbows on fibronectin, but more randomly on mAb13. In addition, MDA-MB-231 cells on fibronectin-coated micropatterns were imaged to observe possible cell type specific differences. Compared to experiments on fixed cells, the live-imaging was expected to reveal if the direction of front-rear polarization is a static condition or constantly under changes, especially with mAb13-coating, which had led to more random polarization of the U-251 MG cells.

Tracking centrosomes and nuclei produced tabular data describing the position of the centrosomes relative to mass center of the nuclei (with x and y coordinates), the speed and mean speed of the centrosomes, the area and mean area of the nuclei, the speed and mean speed of the nuclei, as well as nucleus-centrosome vectors (direction and length with x and y coordinates). Interestingly, there were no significant changes in the speed of the nuclei or centrosomes, nuclear area or nucleus – centrosome vector length between the U-251 MGs on fibronectin or mAb13 and MDA-MB-231s on fibronectin. (data not shown).

Circular histograms were created to visualize the data (Figure 10). For creating the circular histograms, the average direction of polarization of each cell was calculated. One data point represents one cell. Again, fibronectin-coated micropatterns were highly efficient in directing the front-rear polarization towards the wider edge of the micropatterns, whereas using mAb13-coated micropatterns led to more random directions of front-rear polarization. Also,

less cells attached and spread on mAb13-coated micropatterns, compared to fibronectin-coated micropatterns. Visualizing the data emphasized especially the difference of MDA-MB-231 cells on fibronectin to the other study groups.

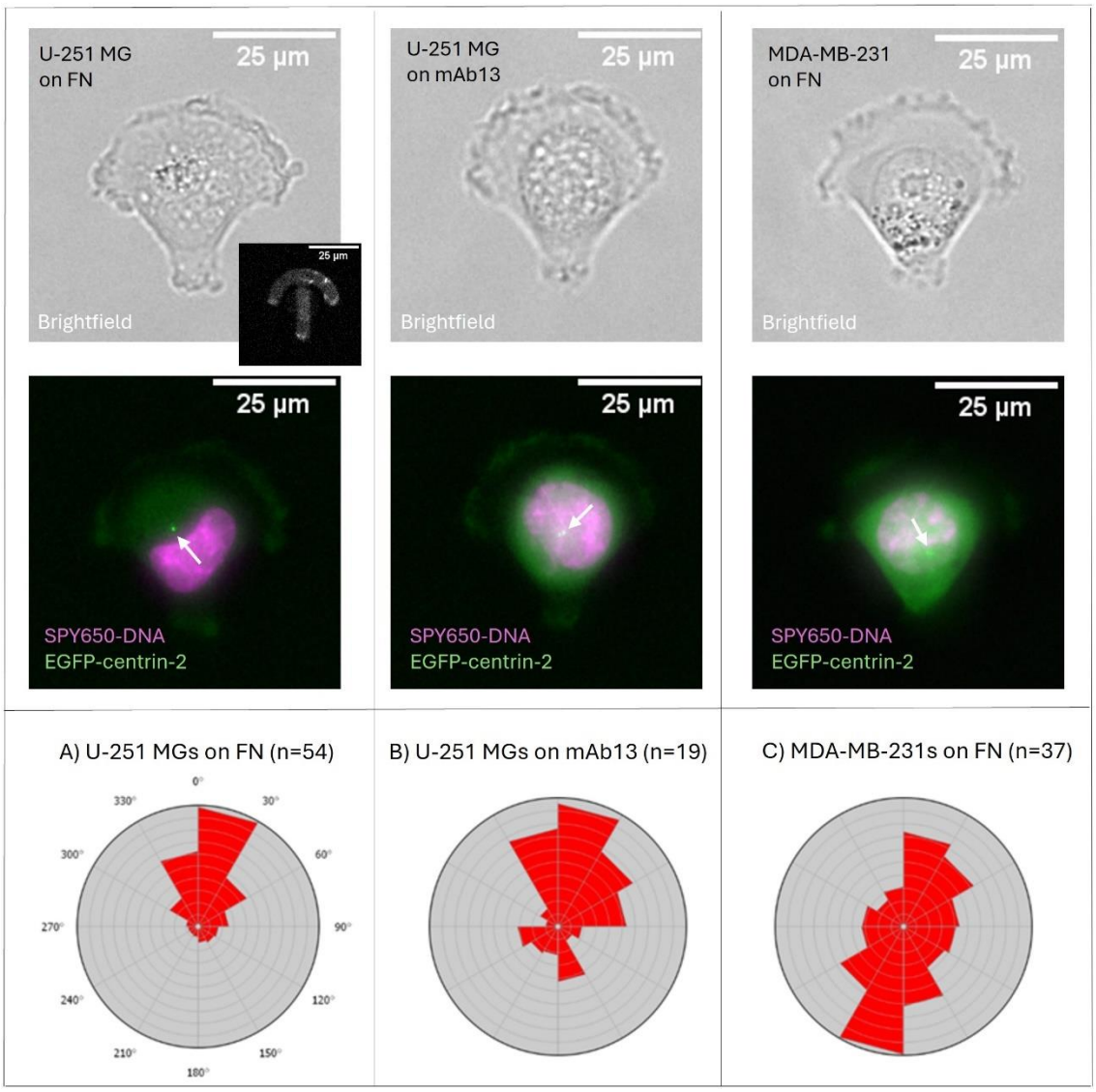

Figure 10. Front-rear polarization of U-251 MG cells on fibronectin and mAb13, and MDA-MB-231 cells on fibronectin-coated crossbow-shaped micropatterns. The cells were imaged every 5 min for 3 hours. At top is presented an example cell for each condition. Both cell lines were transfected with a plasmid to stably express EGFP-centrin-2 for visualization of the centrosomes, and the nuclei were visualized with SPY650-DNA. The centrosomes are annotated with white arrows, with the direction of the arrow representing an estimation of the direction of the nucleus-centrosome vector. Scale bar is 25 µm in all images. The average directions of polarization were calculated for each cell and are here presented as circular histograms. Live-imaging confirmed that geometric control of front-rear polarization depends on protein coating composition and cell type.

The cells were considered polarized towards the front if their nucleus – centrosome vector stayed within ± 60 ° of pointing up towards the wider edge of the crossbow-shape for over half of the time points (19 out of 37 time points) imaged. With this approach, the percentage

of cells polarized towards the front in each group was: 72 % of U-251 MGs on fibronectin (39 of 54 cells), 37 % of U-251 MGs on mAb13 (7 of 19 cells) and 32 % of MDA-MB-231s (12 of 37 cells) (Figure 11.).

In addition, when observing all the time points as single data points, the results were similar as if observing how individual cells were polarized in majority of the time points (as described above). When observing all the time points as single data points U-251 MGs on fibronectin were polarized in expected direction in 69 % of the datapoints (1383 / 1998), U-251 MG on mAb13 in 38 % of the data points (264/703) and MDA-MB-231s on fibronectin in 32 % of the data points (440/1369).

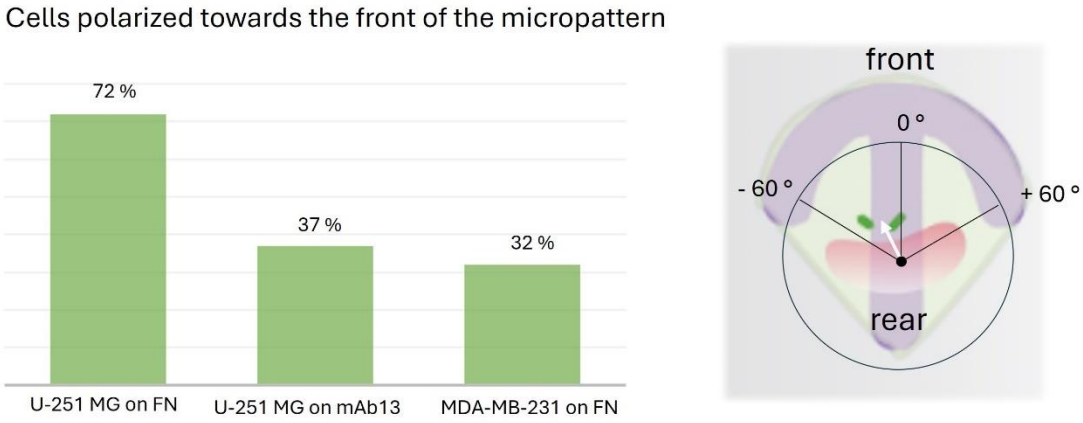

Figure 11. The cells were considered polarized towards the front if their nucleus – centrosome vector was ± 60° of pointing up towards the wider edge of the crossbow for over half of the time points imaged. The relative proportion of cells polarized towards the front in each group was: 72 % of U-251 MGs on fibronectin (39 of 54 cells), 37 % of U-251 MGs on mAb13 (7 of 19 cells) and 32 % of MDA-MB-231s (12 of 37 cells). The fibronectin-coated crossbow-shaped micropatterns were relatively efficient in controlling the direction of U-251 MG cell polarization, whereas on mAb13-coated micropatterns the proportion of cells polarized towards the front (37 %) was only slightly higher than random (360°/120°*100%= 33 %). The proportion of MDA-MB-231 cells polarized towards the front was only 32 %, which indicates a random distribution.

Furthermore, these experiments enabled making other interesting observations. Live-imaging captured how cells attach and spread on the micropatterns, step-by-step (Figure 12. A). Interestingly, some cells could be spotted forcibly retracking on their micropattern and then spreading back to the given pattern-shape (Figure12. B). Moreover, visual inspection of the cells suggested that the direction of cell polarization (nucleus-centrosome vector) was not rapidly changing in any of the study groups. However, whereas the centrosomes were rather static in the middle of the observed cells, and nuclei static or moving only little, the

membrane ruffles of the cells were discovered typically circulating fast at the cell edges in a wave-like motion (Figure 12. C). Furthermore, adhered U-251 MG cell could be spotted blebbing but not undergoing apoptosis (Figure 12. D).

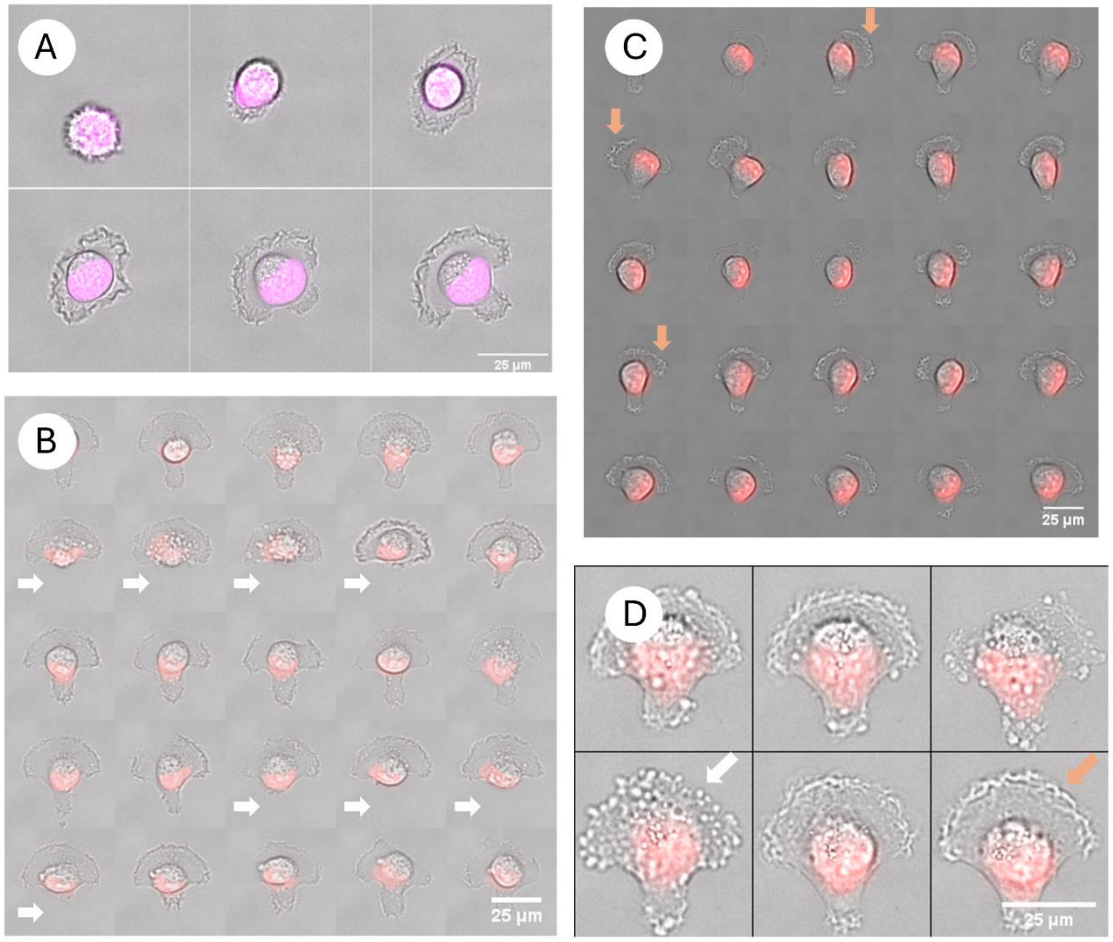

Figure 12. Live-imaging allowed making interesting observations of U-251 MG cell behavior on mAb13-coated crossbow-shaped micropatterns. A) Live-imaging showed step-by-step how cells attach and spread on the micropatterns. B) Some cells could be seen forcibly retracking and spreading back on the micropattern. The “disappeared” cell rear annotated with white arrows. C) The ruffle of the U-251 MG cells could be seen actively traveling around the cell. Annotated with orange arrows. D) An example of a U-251 MG cell on mAb13 blebbing but not undergoing apoptosis. Blebbing wide edge of the cell annotated with white arrow. Ruffling actin cortex annotated with orange arrow. All images are merged images showing brightfield for cell edges and immunofluorescence staining of nuclei with SPY-650 (red / magenta). In montage images A, B and C are shown time-lapse imaging every 5 minutes. In montage image D, time-lapse imaging is shown every 20 minutes.

2.3.3 Linking the direction of migration to the cell front-rear polarization

After we were satisfied with the micropatterning quality and the live-cell imaging conditions, we wanted to move to exploiting the dynamic property of the method to explore how cells behave at the onset of migration, how it is affected by the ability of the cells to polarize or

when they need to switch using a different integrin ligand. We were also interested in observing possible cell type specific differences.

To do so, we started with the same three study groups on crossbow-shaped micropatterns as when live-imaging cell polarization; 1. U-251 MGs on fibronectin coated micropatterns, 2. U-251 MGs on mAb13 coated micropatterns and 3. MDA-MB-231s on fibronectin coated micropatterns, again using stably EGFP-centrin-2-expressing cells. After the cells had adhered to the micropatterns and adopted their shape, they were released to migrate by supplementing the medium with streptavidin-conjugated fibronectin and tracked over time.

Cell migration is often observed by tracking nuclei. However, we wanted to gain information specifically on the cell spreading and direction of migration on the onset of cell migration, and therefore decided to track cell outlines, instead of tracking nuclei. Regrettably, fluorescent Cell Tracker Dye was not distributed in the cells evenly enough to stain the thin cell edges, and the cell edges needed to be tracked from the brightfield images which could not be automated during this project.

When starting to image, I searched and saved areas containing as many successfully transfected cells as possible. Imaging height was adjusted for each field of view accordingly, accompanied with autofocus. Autofocusing took some time with each field of view, but it was still possible to image several focal planes of about 10 fields of views every 5 minutes using up to four channels including brightfield and fluorescent channels. Micropatterning ensured that the transfected cells were still in the saved locations when finishing preparations for the live-imaging session and starting to capture images.

Despite the attempts to optimize the live-imaging conditions, the MDA-MB-231 cells' viability seemed unfortunately to be compromised in the experiments, and therefore they needed to be excluded from the analysis. Thus, instead of the three originally planned study groups, I focused on the differences between the U-251 MGs migrating from either fibronectin or mAb13-coated micropatterns to fibronectin.

It was observed that after the streptavidin-conjugated fibronectin was applied, the U-251 MGs on both fibronectin and mAb13 started quickly to spread to their final size and migrate around the micropatterns. Many of the cells had migrated completely away from their micropattern already during the first hour. In contrast, other cells spread to their full size and actively explored their surroundings in all directions, with lamellipodia ruffling around the cell and

formed small protrusion here and there but did not leave their starting spot. (Figure 13.) In four hours, many of the migrating cells had also reached their neighbors, changing the initial direction of the migration after the encounter. During this time-period, it was even more emphasized, how a small portion of the cells were much more motile and persistent in their migration behavior than the majority of the cells. (Figure 14.)

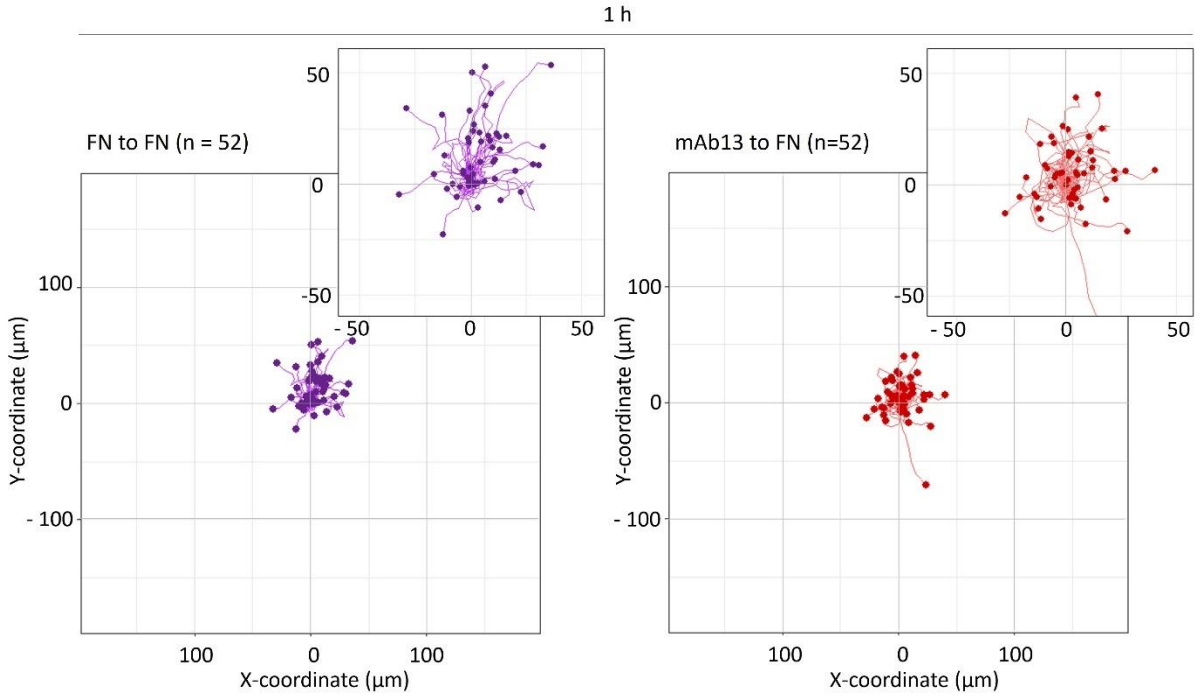

Figure 13. Tracks describing the direction and distance of cell spreading and migration of U-251 MG cells from crossbow-shaped fibronectin- (FN) or mAb13-coated micropatterns to streptavidin-conjugated fibronectin during the first hour. The cells were tracked from 10 min before adding the streptavidin-conjugated fibronectin to 1 h after, at 5min intervals. U-251 MGs started quickly to spread to their final size and migrate around the micropatterns after the streptavidin-conjugated fibronectin was added. Origo (0,0) represents the starting position of the cell (on the micropattern) with the crossbow-shaped micropattern pointing up towards the y-axis. The data was collected from three (Fn) and four (mAb13) independent experiments.

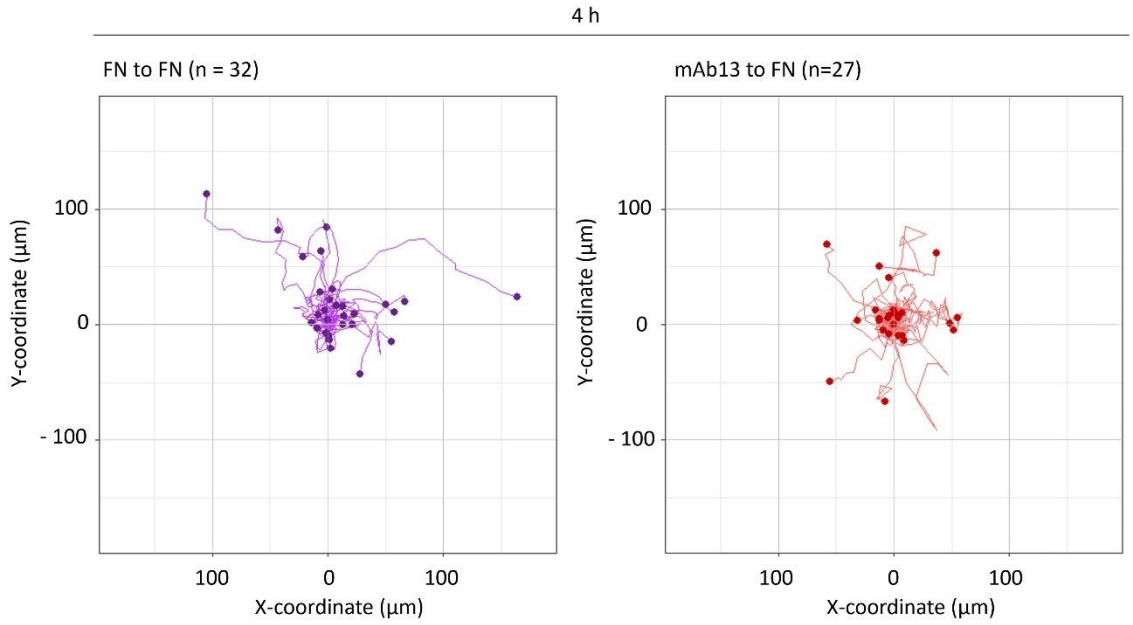

Figure 14. Tracks describing the direction and distance of cell spreading and migration of U-251 MG cells from fibronectin- (FN) or mAb13-coated micropatterns to streptavidin-conjugated fibronectin. during the first four hours. The cells were tracked starting from 10 min before adding the streptavidin-conjugated fibronectin to 4 h after adding the streptavidin-conjugated fibronectin at 15 min intervals. In four hours, it was emphasized, how a small portion of the cells were much more motile and persistent in their migration behavior than the majority of the cells. Also, many of the migrating cells had reached their neighbors and had to be excluded from the analysis. Origo (0,0) represents the starting position of the cell (on the micropattern) with the crossbow-shaped micropattern pointing up towards the y-axis. The data was collected from three (FN) and four (mAb13) independent experiments.

2.3.4 Western blotting was used to study differences in cell signaling between cells attaching to different protein surfaces

Besides observing cell behavior with dynamic micropatterning experiments, we sought to acquire more information about differences in cell signaling when induced by different integrin ligands and/or integrin clustering. Hence, U-251 MG cells were seeded on different integrin-binding ECM components and anti-integrin antibodies including fibronectin, collagen I, 12G10 and mAb13. After the cells had attached and spread, they were lysed and analyzed with Western blotting using immunofluorescent detection. The experiments were performed in presence of fibronectin depleted FBS, as would be during the micropatterning experiments, and additionally, for starved U-251 MG cells.

Initially tested plastic cell culture well plates were not efficient enough to bind the proteins, especially the antibodies, leaving only few cells attached and many floating. This problem

had not occurred with the micropatterning experiments where instead of the cell culture plastics the protein surface coating was prepared on UV-irritated PLL-g-PEG -coated glass. To overcome this problem, I tested coating the cell culture dishes with PLL to enhance the protein binding to the surface. However, the technical control, the wells with no other protein coating but BSA-blocking, revealed that with PLL-coated plastic, BSA blocking was not sufficient to prevent unspecific binding of proteins. Next, I tested polystyrene (PS) cell culture well plates and found them to be appropriate for our experiments. With PS cell culture well plates the U-251 MG cells attached nicely to fibronectin, collagen I, mAb13 and 12G10 -coated wells, but not to the BSA-wells.

Next, I determined the relative proportions of phosphorylated FAK (Y397), Akt (S473) and Erk 1/2 (T202/204) of cells on different integrin ligands compared to total FAK, Akt and Erk 1/2, respectively. As with micropatterning experiments, the cells on fibronectin were considered a positive control group, since on the fibronectin the U-251 MG cells attach efficiently using integrins. The phosphorylation ratios of cells on other integrin ligands were compared to the phosphorylation ratios of U-251 MG cells on fibronectin. As a technical control, the cells were seeded on BSA, which does not support cell adhesion. As a negative control, the cells were kept in suspension to represent baseline expression of proteins of interest when integrin-induced cell signaling is not initiated by cell-ECM binding.

The control groups behaved as expected. The phosphorylation ratios of FAK, Akt and Erk were significantly higher in cells adhered on fibronectin, which was the positive control, than in cells in suspension, which was the negative control. As an exception, the difference was not statistically significant in Akt phosphorylation, where the variance in phosphorylation ratios were big.

As expected, the biggest differences in cell signaling were observed between the cells on fibronectin and the cells on the anti-integrin antibodies. Although, the statistical power of the used nonparametric Kruskal-Wallis test combined with Dunn’s multiple comparison was not enough to verify this, the phosphorylation ratios of FAK and Akt of cells on both anti-integrin antibodies seemed to be lower than of cells on fibronectin. The differences in the phosphorylation ratios were less obvious with Erk phosphorylation, and between cells on fibronectin and on collagen. To find statistically significant differences in the phosphorylation ratios, more replicates could be analyzed, or another quantitative method such as enzyme-linked immunosorbent assay (ELISA) could be implemented. (Figure 15.)

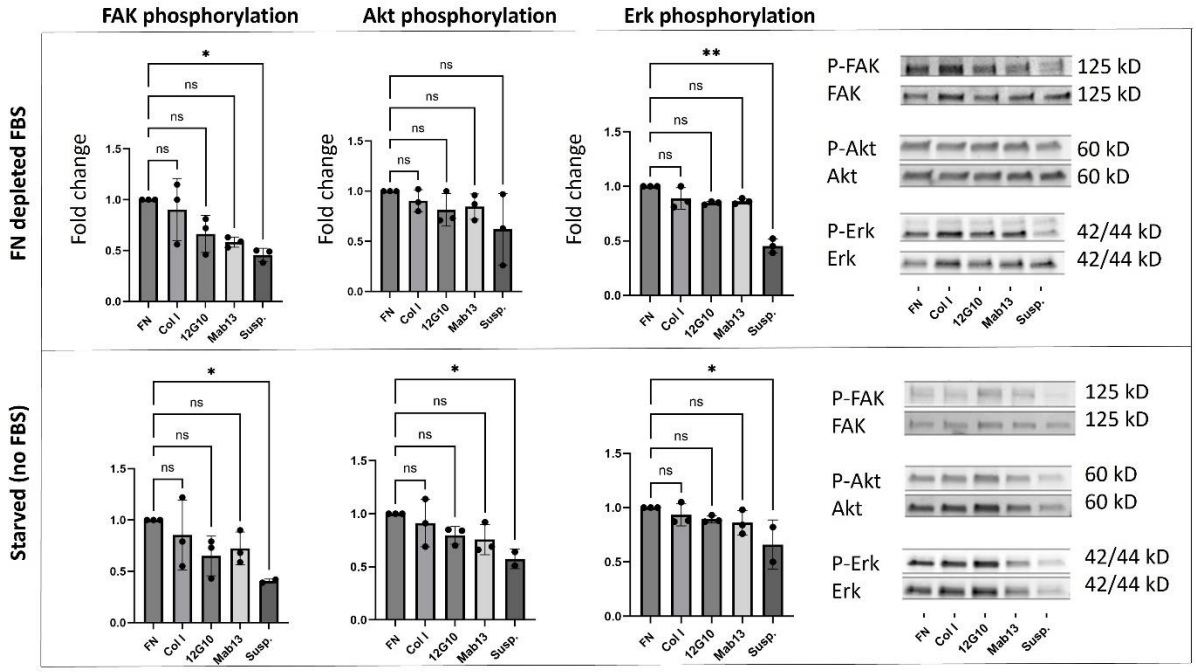

Figure 15. U-251 MG cell signaling on different integrin ligands compared to U-251 MGs on fibronectin. U-251 MGs were seeded on different ECM components and anti-integrin antibodies, including fibronectin (Fn), collagen I (Col I), 12G10 and mAb13, to investigate differences in the phosphorylation ratios of FAK (P-FAK Y397 / FAK), Akt (P-Akt S473 / Akt) and Erk (P-Erk T202/204 / Erk) compared to the cells on fibronectin. Additionally, U-251 MGs were kept in cell suspension (Susp.) as a negative control. With Kruskal-Wallis test and subsequently using Dunn's multiple comparison test, statistically significant differences (*p<0.05, **p<0.01) were found only between the positive and the negative control (fibronectin and cell suspension).

3 Discussion

Micropatterns provide an opportunity to control the distribution of proteins and cells in micrometer resolution. In cell research, they can be used to study single isolated cells and control their microenvironment's e.g., shape and ECM composition. With dynamic micropatterning, the patterning can be modified in the middle of the experiment. Accordingly, the single isolated cells can be released to spread and migrate from the micropatterns in a controlled and standardized manner. This feature can be utilized in analyzing dynamic cellular activities, like cell polarization and migration in normal development and tissue renewal, as well as in pathological conditions such as cancer metastasis.

In this thesis project, a novel low-cost, easily accessible method for producing dynamic micropatterns in cell research laboratories is introduced and its suitability for single-cell studies in academic basic research is investigated. Furthermore, the method for dynamic micropatterning is utilized to study the role of different ECM components and anti-integrin antibodies in supporting front-rear polarization and directed single-cell migration.

3.1 A novel method for dynamic micropatterning was introduced

3.1.1 Coating efficacy, specificity and overall micropatterning quality

The coating efficiency of streptavidin-conjugated fibronectin on biotinylated PLL-g-PEG was visualized using an anti-fibronectin antibody and a secondary antibody linked with a fluorescent label. It could be seen that the coating concentration increased when using more concentrated dilutions. It also seemed that the surface might start to saturate already when coated with concentration of 15 µg / ml streptavidin-conjugated fibronectin. An even more accurate quantification of coating efficacy could be pursued with more data points.

Imaging MDA-MB-231 cell attachment on lines of UV-irradiated and non-irradiated micropatterns confirmed that due to the biotin's high binding affinity to streptavidin, streptavidin-conjugated secondary ligands together with biotinylated PLL-g-PEG can be used to modify specifically the non-irradiated areas, creating two discrete protein coating compositions.

Variation in the quality of micropatterning could be seen in each cover glass, and it might be inevitable with manual micropatterning techniques. The quality of micropatterning was often compromised in the edges of each glass. Therefore, in some test settings, it could be

beneficial to set quality standards to ensure that the effect of micropatterning on the cell behavior is comparable between each micropatterned area (e.g., acceptable variation in imaged intensities of micropatterns, or acceptable maximum micropattern intensity to background intensity ratio). Here, the micropatterns ability to control the cell shape was used as a sign of a successful micropatterning.

Over time, the adhesive patterns can be degraded, and therefore become less adhesive. Fluorescent imaging suggested that U-251 MG cells degrade or modify the protein coating relatively fast, either by degrading or tearing the protein coating, or at least by detaching the fluorescent labelling. Despite the noticed change in micropattern intensity, the patterns were still successful in controlling the cell localization and shape Also, although we used cell culture medium supplied with fibronectin depleted serum, it should be noted that remains of fibronectin may still exist, and the medium can contain small amounts of integrin ligands. In addition, cultured glioblastoma cells have been reported to produce basement membrane components including fibronectin, collagen I, laminin and vitronectin [Seker-Polat et al., 2022]. Therefore, using appropriate and standardized attachment times before imaging is critical, especially when studying the impact of different ECM proteins on cell behavior. Indeed, Fink et al. came to a similar conclusion, when they tested several already published micropatterning techniques with a few different cell lines: HeLa cells, RPE1 cells and mouse embryonic fibroblasts. They noticed that the tested cell types varied from each other in terms of their ability to rip off the patterned proteins and to escape from the patterns. [Fink et al., 2007] Fascinatingly, Tseng et. al. used fibrinogen-Alexa 546 coating to measure micropattern deformation and noticed that micropattern deformation could be utilized as a tool to measure cell traction forces [Tseng et al., 2011].

Although we were satisfied with the micropatterning quality, possible improvements can always be considered. E.g., it could be tested whether washing the glass coverslips by dipping and shaking would result in more efficient washing and more even protein coating. Additionally, although not necessary, carrying out all the steps of micropatterning in completely dust free conditions such as in a clean room or in a laminar hood could be the optimal working environment for achieving the best possible micropatterning quality.

3.1.2 Biocompatibility of the biotinylated PLL-g-PEG for micropatterning purposes

The biocompatibility of the biotinylated PLL-g-PEG for its intended use was ensured by comparing the cell structure and adhesion sites of cells seeded on micropatterned biotinylated

PLL-g-PEG and conventional PLL-g-PEG. Biocompatibility is a major concern when testing new materials for biological applications. No signs of cytotoxicity or even subtle changes in cell structure and adhesion were noticed.

In addition, creating images of average intensities of the fluorescent labelled cell structures served as a beautiful example on how well micropatterns can function in standardizing the research populations of the cells. This ability to standardize the study subjects can e.g. help to discover differences in cell screenings between the treatment groups and enable automatizing the data analysis, and therefore save the researchers' money and / or time.

3.1.3 Imaging conditions and data handling

The centrosomes of fixed cells could be recognized simply by immunofluorescence staining of γ-tubulin. Also, colocalization of paxillin with the centrosome was observed, as previously reported [Dubois et al., 2017], and found to be helpful in detecting the centrosome in otherwise uncertain cases. Transfection of the cells with plasmid DNA enabled tracking the fluorescent protein-containing centrosomes in living cells over time. In both cases, several focal planes of the cells needed to be imaged to ensure that the centrosome was caught in the focus while the cells were moving.

Transfection, cell sorting, membrane and DNA dyes, antibiotics, centrifugation, and all handling procedures performed outside of the optimal culture conditions of a cell incubator, can cause stress to the cells. Especially phototoxicity during lengthy imaging sessions was recognized as a risk factor for the viability of the cells. Ideally, all the cells would have the same expression levels of GFP and each dye to ensure that the amount of phototoxic stress for cells is similar in the whole research population. Cell sorting of GFP positive cells into two groups (cells with medium expression and cells with high expression of EGFP-centrin-2) decreased the variability between the cells.

Tracking the cell edges from fluorescent imaging was considered as the primary option, since it can be easily automatized. Unfortunately, the fluorescent dye intended for monitoring cell movement or location, was not distributed evenly enough in the cells, leaving the thin cell edges almost stainless, which interrupted the automatic cell edge detection. However, the cell edges could be easily recognized by eye from brightfield images. Manual drawing of the cell edges from these images was a rather laborious and time-consuming method, but beneficial for decreasing the amount of phototoxicity and stress for the cells.

Imaging can be tedious to quantify, and at least partial automatization of the image analysis pipeline was considered as necessary. Development of machine learning and artificial intelligence are expected to ease the image analysis and data handling in the following experiments, and to make live-imaging more accessible and efficient tool for cell biology research, and its applications.

3.2 The role of integrin ligands in geometric control of U-251 MG and MDA-MB-231 cell polarization and migration with dynamic micropatterning

It has been demonstrated that cells on crossbow-shaped micropatterns adopt a distinctive front-rear polarity with the cells positioning their centrosome and the Golgi in front of their nucleus, towards the wider edge of the adhesive micropatterns [Théry et al., 2006]. I investigated whether this is influenced by the specific adhesive substrate the cells are adhering to. I plated U-251 MGs on micropatterns coated with common ECM components (integrin ligands) including fibronectin, collagen type I, vitronectin and laminin-521. In addition, U-252 MGs were plated on micropatterns coated with anti-integrin β1 antibodies mAb13 and 12G10. Then, after fixing, I determined the cells' front-rear polarity by immunofluorescence staining.

My data indicated that when adhering to fibronectin and laminin, the U-251 MG cells highly consistently oriented their MTOC towards the wider edge of the crossbow-shaped micropatterns, whereas in cells plated on collagen, vitronectin, inactivating anti-integrin β1 antibody mAb13 or activating anti-integrin β1 antibody 12G10, the direction of polarization was less consistent. These observation were later confirmed, when the data were pooled with two other independent repetitions of the experiment, and investigated with statistical testing. [Isomursu et al., 2024]. As an exception, it was left unclear how well the vitronectin-coated micropatterns can control the direction of U-251 MG cells front-rear polarization, since the data from independent experiments was inconsistent.

By visual inspections, with both antibodies there were less attached cells and less fully spread crossbow shaped cells than with ECM components. Also, more double-occupied micropatterns were observed. It seemed that the cells were attaching to each other when having difficulties in attaching to the micropatterns. Therefore, it could be expected that compared to the cells on fibronectin, the geometric control of cell polarity was weaker when the micropatterns were coated with either of the antibodies.

Surprisingly, by visual inspection, I observed less attached and fully spread cells on 12G10-coated micropatterns than on mAb13-coated micropatterns. However, we still chose to concentrate in the dynamic micropatterning experiments to compare cells on fibronectin and mAb13 due to their expected differences in integrin activation and impact on cell signaling.

3.2.1 Dynamic micropatterning revealed substrate and cell type specific differences and similarities in the onset of migration from crossbow-shaped micropatterns

Next step towards utilizing dynamic micropatterns in my research was to live-image the dynamics of front-rear polarization of U-251 MGs on crossbow-shaped micropatterns before releasing them to migrate. Here we focused on the differences of U-251 MGs seeded on fibronectin and mAb13 -coated crossbow-shaped micropatterns. Again, the direction of front-rear polarization was more consistent on fibronectin-coated crossbows than on mAb13-coated crossbows. In addition, unlike with the U-251 MGs, the fibronectin-coated crossbow-shaped micropatterns could not control the direction of front-rear polarization of MDA-MB-231 cells. This was an interesting finding since Mahmud et al. (2009) had observed in their micropatterning experiments that MDA-MB-231 cells polarized and spread towards the wider edge of adhesive patterns shaped like connected triangles [Mahmud et al., 2009]. However, the finding is not in direct contrast with the results of Mahmud et al. Although the cell shape on crossbow-micropatterns and triangles may look similar, as Thery et al. (2006) reasoned, the crossbow-shape is unique in creating non-adhesive sides. Also, the surface area and dimensions of the micropatterns are a crucial factor in geometric control of the cell front-rear polarization.

Finally, I studied how the onset of U-251 MG migration to fibronectin is affected by whether the cells start their journey from fibronectin or mAb13-coated crossbow micropatterns. Additionally, I studied MDA-MB-231 cells released from fibronectin-coated micropatterns to fibronectin. Regrettably, MDA-MB-231 cells seemed to be more sensitive to phototoxicity of the imaging conditions than the U-251 MGs and had to be excluded from the data analysis.

Firstly, these experiments demonstrated that streptavidin-conjugated proteins bind to biotin rapidly, and the modification of the micropatterns is therefore almost instant, with no long incubation times needed. Therefore, the method is suitable for studying the early events of migration and spreading while keeping the cells under live-imaging conditions the entire time. Secondly, tracking the migration paths of U-251 MGs leaving from fibronectin and mAb13

showed that in both conditions the majority of the cells spread and moved towards the wider edge of the crossbow-shaped micropatterns.

As planned, later also the direction of the cell front-rear polarity of these migrating cells was determined and studied by the host laboratory. It was found that the centrosome orientation was not effective in predicting the direction of cell spreading and migration from the micropatterns, especially with the U-251 MGs migrating from fibronectin-coated micropatterns to fibronectin. Instead, there was observed a correlation between higher directional persistence and consistent centrosome orientation toward the leading edge after the cells had been released to migrate. The findings supported the idea that centrosome reorientation toward the nascent lamellipodium may help to stabilize polarized trafficking and protrusion, promoting directional cell migration in U-251 MG cells. [Isomursu et al., 2024]

3.2.1 U-251 MGs were actively blebbing on micropatterns, but did not undergo apoptosis

In our experiments, some of the U-251 MG cells were observed to form blebs, spherical cellular protrusion in the cell membrane that are generated by hydrostatic pressure, without undergoing cell death. Blebs have been considered long as a hallmark of apoptosis, but also typical for cell migration in low-adhesive environments [Paluch and Raz, 2013]. Furthermore, recent discoveries suggest that in low-adhesion environments, blebs help cancer cells avoid programmed cell death by assembling oncogenic signaling hubs [Weems et al., 2023].

It is cell type specific if the cells have the ability to switch between different migration strategies and utilize blebbing in their migration, alone or in combination with other protrusion types such as actin-polymerization driven lamellipodia formation [Paluch and Raz, 2013]. Blebbing in viable U-251 MG cells was an interesting observation since, as stated before, glioblastoma cells are believed to specifically migrate individually with a mesenchymal mode of migration [Zhong et al., 2010], using strong cell-ECM adhesions. Only little is known of the mechanisms and causality between blebbing and directed migration in adhesive cell environments. However, in 2011 Oppel et al. reported that they found that glioma cells may be able to switch to protease-independent amoeboid migration when their means to mesenchymal migration are disturbed [Oppel et al., 2011]. Soon after, Weeks et al. verified that in certain circumstances, glioma cells may undergo mesenchymal-amoeboid transition (MAT) and therefore are capable of migrational plasticity [Weeks et al., 2012]. Still, the role of amoeboid migration in glioma metastasis *in vivo* remains largely unknown.

Interestingly, Bergert et al. (2012) showed with micropatterned Walker 256 carcinosarcoma cells, that shifting the balance between actin protrusivity and actomyosin contractility, as well as changes in substrate adhesion, can induce switches between blebs and lamellipodia without any change in cell shape and polarity. Moreover, they suggested that the mechanisms underlying cell polarity are similar in bleb- and lamellipodia-forming cells. [Bergert et al., 2012]

In the future, micropatterns could be used to study the effect of different ECM components on blebbing and migration behavior of U-251 MGs and different cancer cell types. Addressing this topic would require a plan for a data analysis pipeline to visualize and quantify the results.

3.2.2 Different integrin ligands can be utilized to manipulate cell signaling and cell behavior

To investigate differences in cell signaling when induced by different integrin ligands and/or integrin clustering, U-251 MGs were seeded on different ECM components and anti-integrin antibodies, including fibronectin, collagen I, 12G10 and mAb13. Then, phosphorylation ratios of FAK, Akt and Erk were determined and compared to the corresponding phosphorylation ratios of the cells on fibronectin. As expected, the biggest differences in cell signaling were observed between the cells on fibronectin and the cells on the anti-integrin antibodies. Regrettably, the differences in the phosphorylation ratios were not statistically significant, expect with the positive and negative control.

Integrin activation and aggregation at ECM interaction sites induces FAK phosphorylation and initiates recruitment of different intra-cellular proteins, which are needed for formation of mature integrin mediated adhesions such as focal adhesions. FAK is a central component of these adhesions and responsible for recruiting cytoskeletal proteins and activating Rho GTPases, playing a crucial role in controlling cell attachment, reorganization of the actin cytoskeleton, cell front-rear polarity and migration. [Hu et al., 2024; Katoh, 2020] FAK is overexpressed in many types of tumors, including gliomas, and its increased expression correlates with cancer invasiveness and recurrence [Seker-Polat et al., 2022; Wang et al., 2019]. Furthermore, FAK is a crucial regulator of PI3K/AKT and Ras/MEK/ERK pathways. The PI3K/AKT and Ras/MEK/ERK pathways are known for being central transducers of oncogenic signals and their dysregulation contributes to the pathogenesis of various cancers.

[Asati et al., 2016; Jokinen et al., 2012] In the experiments of this thesis, measuring phosphorylated AKT and ERK offered information of the activation of these pathways.

Targeting FAK and individual components of the PI3K/AKT and Ras/MEK/ERK pathways are already recognized as potential drug targets in cancer therapy [Mustafa et al., 2021; Pang et al., 2021]. As typical in drug development, many of them have been promising in preclinical models, but fewer in actual patients. Still, attempts to develop pharmaceuticals to prevent cancer cell invasion and metastasis by targeting oncogenic pathways related to cell adhesion, matrix degradation, and cytoskeletal rearrangement are ongoing. Currently ongoing clinical trials include e.g. trials on FAK inhibitors ifebemtinib (NCT06166836) and defactinib (NCT05798507). Also, MEK inhibitor binimetinib is currently being studied as a repurposed agent to treat low-grade glioma in children (NCT02285439). (Retrieved from clinicaltrialrials.com on 28th of Seb in 2024)

My findings together with earlier studies show that cell signaling and behavior can be manipulated with different integrin ligands and other compounds targeting integrin-induced cell signaling. Targeting the processes of cell front-rear polarization and migration with new pharmaceuticals attracts with the possibilities to apply the new findings to all kinds of metastasis-forming cancers. However, lessons should be learned from past mistakes. It seems that successful inhibition of cell migration might need a cocktail of molecules to target multiple cell signaling pathways at once, and prevent both the mesenchymal and amoebic migration modes [Friedl and Wolf, 2003; Raudenská et al., 2023]. Dynamic micropatterning can offer a new tool to investigate and understand how cells react to external chemotactic signals and how cell polarization and migration are affected when certain cell signaling pathways are targeted with inhibitors.

3.3 Ethical principles and research integrity

This thesis followed good research practices and a responsible research culture in accordance with European research ethics guidelines and institutional guidelines, where reliability, honesty, respect and accountability are considered the basic principles of research integrity.

4 Conclusions

With dynamic micropatterning, areas between micropatterns, which are biologically inert, can be made permissive for cell-substrate adhesion, and thus cells on micropatterns can be released to migrate and create new cell-substrate and cell-cell connections in a controlled and standardized manner. Techniques for dynamic micropatterning facilitate the studies of how cells react and fine-tune their behavior in response to changes in their microenvironment and, thus, help us to visualize and understand the biological mechanisms of dynamic cellular activities, such as cell polarization, adhesion and migration in both normal development and tissue renewal, as well as in pathological conditions.

In this thesis project, biotin-streptavidin binding was utilized to introduce a novel low-cost, easily accessible method for producing dynamic micropatterns in cell research laboratories. This method can be used to achieve a good micropatterning quality in academic basic research, while minimizing expensive specialized devices and techniques.

As a first step of method optimization and validation, I studied the coating efficiency of secondary ligand on biotinylated surfaces in four different concentrations with immunofluorescence detection. My results indicate that the amount of the streptavidin-conjugated ligand is scalable in a controlled manner. To demonstrate the specificity of the streptavidin-biotin bond in controlling ECM protein placement on and off the photopatterned regions, I imaged the cell adhesion sites of MDA-MB-231 cells, a human breast cancer cell line, grown on micropatterns of narrow lines.

To ensure that the modified surfactant does not influence the morphology of the micropatterned cells, I imaged U-251 MG human glioblastoma cells' actin cytoskeleton and paxillin-positive adhesions on fibronectin-coated crossbow micropatterns manufactured on PLL-g-PEG and biotinylated (50%) PLL-g-PEG surfaces. My data indicates that cell adhesions and cell morphology were similar on micropatterns generated with both anti-fouling agents: on the biotin-conjugated PLL-g-PEG as well as on the conventional (i.e., unconjugated) PLL-g-PEG surface coating.

It has been shown that cells on crossbow-shaped micropatterns adopt a distinctive front-rear polarity towards the more adhesive edge of the micropattern [Jiang et al., 2005; Théry et al., 2006]. I investigated whether this is influenced by the specific adhesive substrate the cells are adhering to. I plated U-251 MGs on micropatterns coated with common ECM components

(integrin ligands) including fibronectin, collagen, vitronectin and laminin, and on monoclonal anti-integrin antibodies mAb13 and 12G10, and determined their front-rear polarity based on immunofluorescence staining of nuclei and centrosomes of the fixed cells. Indeed, the cell front-rear polarization on crossbow-shaped micropatterns varied depending on the integrin ligand used for protein coating. Micropatterns with fibronectin and laminin were highly efficient in controlling the direction of U-251 MG front-rear polarization, whereas using collagen, vitronectin, mAb13 and 12G10 led to bigger variation in the directions of the cells' front-rear polarity.

The dynamics of the cell front-rear polarization on crossbow-shaped micropatterns were further studied with live-imaging of U-251 MG cells on either fibronectin or mAb13 -coated micropatterns, and MDA-MB-231 cells on fibronectin-coated micropatterns. Again, when adhering to fibronectin, the U-251 MG cells preferentially oriented towards the wider edge of the micropatterns, whereas in cells plated on inactivating integrin β1 antibody mAb13, the direction of polarization was less consistent. I also observed that the ability to adopt front-rear polarity varies between cell types. MDA-MB-231 cells were not polarized by the fibronectin coated crossbow shape.

Finally, the front-rear polarization and its effect on the direction and persistence of cell migration was investigated with dynamic micropatterning. In these experiments my aim was to determine whether cell behavior at the onset of migration is affected by the adhesive ligand and variations in front-rear polarity. To do this, I compared the migration of U-251 MG cells from fibronectin- or mAb13-coated micropatterns to fibronectin. From both fibronectin and mAb13 -coated micropatterns, U-251 MGs started to rapidly spread and migrate after adding the streptavidin-conjugated fibronectin. In this thesis, I have visualized the migration paths. As a continuation to this work, the data was later analyzed further by the host laboratory.

To conclude, my data indicates that the dynamic micropatterning method allows easy single-cell micropatterning with good quality and rapid modification of the surface, enabling investigation of cell dynamics upon their transition from static adhesion to an actively migrating state. The method is relatively easy to adopt in any biomedical laboratory and does not require expensive reagents or specialized equipment. Though, to be fully able to utilize the benefits of this method, at least partial automatization of the data-analysis might be required. However, rarely one solution fits all, and different micropatterning methods should be considered and utilized according to one's study questions.

5 Materials and methods

5.1 Cell culture, transfection, and cell sorting

5.1.1 Cell culture

U251 MG human glioblastoma cells were obtained from Dr. David J. Odde (University of Minnesota), authenticated using a short tandem repeat assay (Leibniz Institute DSMZ – German Collection of Microorganisms and Cell Cultures) and maintained in Dulbecco's modified Eagle's medium (DMEM) /F-12 (Gibco, 11320-074) containing 8 % fetal bovine serum (FBS) (Sigma, F7524). MDA-MB-231 human breast adenocarcinoma cells were purchased from American Type Culture Collection and authenticated using a short tandem repeat assay (DSMZ). MDA-MB-231 (human breast adenocarcinoma) cells were maintained in high-glucose DMEM (Sigma, D5796-500ML) containing 1% MEM nonessential amino acids (Sigma, M7145-100ML), 1% L-glutamine (Sigma, G7513-100ML) and 10% FBS (Sigma, F7524). Both cell lines were cultured on cell culture plates at +37°C, 5% CO2 in a humidified incubator, and routinely tested for mycoplasma contamination.

Fibronectin depleted serum had been previously manufactured by the lab, by separating and removing the serum fibronectin from FBS with liquid chromatography and Gelatin Sepharose 4B resin (Sigma, GE17-0956-01). The resulting fibronectin depleted FBS had been sterile filtered using a 0.22 µm Stericup filter (Merck Millipore, SCGPU05RE) and stored at -20 °C. The success of the fibronectin depletion of the processed FBS had been confirmed by western blotting with anti-fibronectin antibodies.

5.1.2 Transfection

To visualize the centrosome, both U-251MG and MDA-MB-231 cells were transfected with pEGFP-centrin-2 (donated by Dr. Erich Nigg, Addgene plasmid #41147) using Lipofectamine 2000 (Thermo Fisher Scientific, 11668019). For the transfection, the cells were passaged onto wells of a 6-well plate at approx. 40% confluency in 2 ml of medium. The cells were supplemented with 0.5 µg and 1.0 µg of pEGFP-Centrin2 and 1,25 µl Lipofectamine 2000 in 200 µl of Opti-MEM (Thermo Fisher Scientific, 31985070) and incubated at +37 °C/5% CO_2 overnight before changing the culture medium. The cells transfected with 0.5 µg of the plasmid DNA were selected for subculturing based on the amount of transfected viable cells. The cells

transfected with 1.0 µg of the plasmid DNA were discarded. The transfected subpopulations of the cells were then cultured with 400 µg/ml of G418 disulfate salt (Sigma-Aldrich, G8168-10ML), an aminoglycoside antibiotic used as a selective agent for eukaryotic cells, for two weeks to create and maintain a stable transfected cell population for the experiments.

5.1.3 Cell sorting

The percentage of successfully transfected cells was increased by sorting the cells with Sony SH800 Cell Sorter. Additionally, sorting the cells allowed obtaining cell populations with more even expression levels of the green fluorescent protein. With both cell lines, the cells were detached with trypsin, centrifuged as a cell pellet and the supernatant was discarded. The cell pellets were resuspended in 2 % FBS in PBS and pipetted into cell strainer tubes. The cells were kept on ice bath prior to sorting. Cells with medium and high expression of GFP, were collected separately. Sorting of U-251 MG cells yielded approximately 37 000 cells with medium expression, and 45 000 cells with high expression. Sorting of MDA-MB-231 cells yielded around 15 000 cells with medium expression and 13 000 cells with high expression. The sorted U-251 MG cells were first seeded on 6-well plates and MDA-MB-231 cells on 12-well plates before growing confluent enough for passage onto a normal 10 cm cell culture plate.

5.2 Antibodies and reagents

The antibodies and reagents used for immunofluorescence staining and their dilutions were: rbt anti-fibronectin (Sigma F3648) 1:150, rbt anti-paxillin 1:250 (Abcam, 32084), ms anti-γ-tubulin (Abcam, 11316) 1:250, phalloidin-488 (Invitrogen, A12379) 1:100, SiRActin (Tebu-Bio, SiRActin Kit SC001) 1:1000, DAPI (4′,6-diamidino-2-phenylindole) 1:500. Alexa Fluor 555 -conjugated BSA (Thermo Fisher Scientific, A34786, A34785) and Alexa Fluor 647 -conjugated fibrinogen (Thermo Fisher Scientific, F35200) were used for visualizing micropatterns. Alexa Fluor 488/568/647 -conjugated secondary antibodies and their dilutions were: anti rbt 488 (InVitrogen, A21206), 1:200-300, anti-rbt 568 (InVitrogen, A211039), anti-ms 647 (InVitrogen, A31571) 1:200-300. In live imaging, DNA/nuclei were visualized with SPY555-DNA (Spirochrome, SC201) 1:1000 and SPY650-DNA (Spirochrome, SC501) 1:1000.

The antibodies used for Western Blotting and their dilution were: rbt anti-p-FAK (4397) CST/8556 (MW 125 kDa) 1:1000, rbt anti-p-Akt (S473) CST/9271 (MW 60 kDa) 1:1000, ms anti-Akt (pan) CST/2920 (MW 60 kDa) 1:1000, rbt anti-p-ERK (202/204) CST/4370 (MW

42, 44 kD) 1:1000 and ms anti-ERK CST/4696 (MW 42, 44 kD) 1:1000 obtained from Cell Signaling Technologies, and ms anti-FAK BD610088 (MW 125 kDa) 1:1000 obtained from BD Biosciences. The secondary antibodies and their dilutions were: Azure Spectra 650 goat anti-ms (AC2166) 1:2500 and Azure Spectra 800 goat anti-rbt (AC2134) 1:2500 obtained from Azure Biosystems.

Anti-integrin antibodies, clone 12G10 (ms anti-integrin β1 against extended open conformation) and clone mAb13 (rat anti-integrin β1 against closed conformation), used as a substrate for cell adhesion at the indicated concentrations, were in-house production. Other proteins used as substrates for cell adhesion included fibronectin (PromoCell, C-43050), type I collagen (Sigma, C8919), and recombinant human laminin 521 (BioLamina, LN521).

5.3 Micropatterning and sample preparation for imaging

The method to manufacture micropatterns was modified and optimized by the host laboratory from what has been described before by Azioune et al. (2009).

5.3.1 Surface preparation and PLL-g-PEG coating

Before PLL-g-PEG coating, the glass coverslips were cleaned and prepared by acid washing and baking in an ozone producing UV (UVO) oven. Glass coverslips were acid washed in decanter glass by rinsing in a small amount of concentrated nitric acid for 5 min, followed by rinsing under running water and 6 rinses with ultrapure water, a wash in methanol, and lastly, in 97% ethanol. The glasses were left to dry protected from dust and then baked in an UVO oven for 5 min (Jelight Company UVO Cleaner 342-220).

PLL-g-PEG surface was produced by incubating the coverslips upside down in a drop, 13 mm glass coverslips in 20 µl and 22 mm glass coverslips in 60 µl, of 0,1 mg/ml PLL(20)-g[3.5]-PEG(2) (Surface Solutions, Switzerland) in 10 mM Hepes, pH 7.3, for 1 h at room temperature. For dynamic micropatterning, 50% biotinylated PLL(20)-g[3.5]-PEG(2) was used. After incubation, the coverslips were washed twice with PBS and rinsed once with ultrapure water, dried and stored at RT protected from dust.

5.3.2 Surface patterning using photolithography

Controlled UV exposure, from 30 to 33 mW / cm2 at 253,7 nm (Jelight Company UVO Cleaner 342-220), through a chromium and synthetic quartz photomask (Delta Mask,

Netherlands) was used to create adhesive patterns on the PLL-g-PEG surface for the ligands and cells to attach to. Before and after use, the photomask was cleaned by rinsing with ultrapure water and 70 % ethanol, dried using airflow and baked in UVO oven for 5 min.

The glass coverslips were attached to the chrome photomask with a drop of water, allowing close contact between the glass and the photomask. For glasses with a diameter of 13 mm, 6 µl of ultrapure water was used, and for glasses with 23 mm diameter, 12 µl. Excess water from the edges was gently dried with a non-dusting paper. Lastly, a plastic cover was attached to secure the assembly using drops of ultrapure water on the edges of the photomask, around the glass coverslips.

The chrome photomask assembly was then baked in the UV oven upside down allowing the UV light to reach only predefined microscale patterns through the holes of the photomask. The PLL-g-PEG surface areas exposed to UV light treatment form carboxyl groups which contribute to strong binding of proteins, including matrix components such as fibronectin and fibrinogen. Photomasks with different designs were used to create different shapes and sizes of patterns. The patterned coverslips were kept protected from light and dust and stored at +2 – +8 °C for up to one month, or until used.

5.3.3 Protein and cell micropatterning

Coating with matrix proteins was performed by incubating the coverslips upside down in a drop of the protein mixture of interest in PBS on parafilm, for 1 hour at RT in a humidity chamber, followed by washing them twice with PBS. A low concentration of fluorescently labelled BSA or fibrinogen was included in the mixture to enable visualizing the micropatterns with fluorescent microscopy. Thereafter, the coverslips were blocked with 2% BSA in PBS for 30 min at RT and again washed with PBS.

Cells were detached with trypsin and resuspended in their growth media supplemented with fibronectin-depleted FBS. Micropatterned protein-coated cover glasses were placed on the bottom of a cell culture multiwell plate, or in an Attofluor imaging chamber designed for live-cell imaging (Thermo Fisher Scientific), and the cells were seeded on them at approx. 10-20 % confluency to minimize the number of patterns occupied by multiple cells. The cells were left to settle for a short period of time until they could be seen attaching to the patterns. Excess and unbound cells were washed away with the fibronectin-depleted full medium using simultaneous rinse and suction to prevent the attached cells from drying out during the

medium change. After seeding the cells, they were left to settle in the incubator until they were fully spread on the patterns, typically, 3 to 4 hours, before they were fixed or taken into live-cell imaging.

5.3.4 Dynamic micropatterning with streptavidin-conjugated ligands

Streptavidin-conjugated proteins bind strongly and specifically to the biotin, allowing the micropatterned cells to occupy previously non-adhesive areas between the micropatterns. To release the bound cells from the micropatterns and to observe their migration behavior, the culture medium was supplemented with 1 µg/ml of streptavidin-conjugated secondary ligand (e.g., fibronectin) diluted in a small amount (50 µl) of fibronectin depleted medium.

Streptavidin-conjugated fibronectin and GFOGER were manufactured with FastLink Streptavidin Labeling Kit (Abnova KA1556) according to the manufacturer's instructions. The fibronectin was purchased from Merck-Millipore Calbiochem (341631-5MG) and the GFOGER custom helical collagen-mimetic peptide was ordered from Auspep (Product code: CS, Batch No. BE10205).

5.3.5 Fixing and immunofluorescence staining

The cells were fixed with warm 4 % paraformaldehyde (PFA) in the growth medium for 15 min by applying 16 % PFA 1:4 to the growth medium while gently shaking the plate. After fixing, the cells were washed three times with PBS, and permeabilized and blocked with 0.3 % Triton in 10 % horse serum for 20 to 30 min.

The primary antibodies were incubated overnight at 2 – 8 °C and the excess was washed once with 0,05 % Tween 20 in PBS (PBST) and twice with PBS. The primary antibody incubation was followed by incubation with corresponding fluorescent secondary antibodies for approx. 90 min at RT. Excess secondary antibodies were washed twice with PBS and finally once with ultrapure water.

Finally, the glass coverslips were mounted with 6 µl of Mowiol-DABCO, a mixture containing 2.5% 1,4-diazabicyclo[2.2.2]octane (DABCO) (Sigma, D27802) in Mowiol (Merck Millipore, 475904). The mounted glass coverslips were then allowed to rest at RT at least overnight before imaging.

5.4 Method validation

5.4.1 Investigation of streptavidin-conjugated ligand binding to biotinylated PLL-g-PEG with different coating concentrations

To observe the coating efficiency of biotinylated PLL-g-PEG with different streptavidin-conjugated fibronectin concentrations, a series of micropatterned and protein-coated cover glasses were prepared and imaged. Micropatterns of 9 µm wide lines were coated with 15 µg / ml fibronectin and 5 µg / ml BSA-AF555. The area between the patterns was coated with 0, 1, 5 or 15 µg / ml streptavidin-fibronectin (full length) in growth medium (DMEM/F-12).

Before immunofluorescent staining, the coated glass coverslips were washed once with growth medium and once with PBS and blocked for 10 min with 10 % horse serum in PBS to prevent unspecific binding of antibodies.

Of each condition, 6 to 9 fields of view were imaged with spinning disk confocal microscope to detect and measure the signal intensity obtained from immunofluorescence-stained fibronectin. The intensity of the signal was measured with Fiji / Image J from 10 separate areas in each imaged view, approximately in the middle of the image. Then, mean signal intensities were calculated for each coating condition. The background signal was subtracted from the signal / intensities before plotting.

5.4.2 Visualization of MDA-MB-231 adhesion sites with static binary micropatterning

Four kinds of binary micropatterns were created on biotinylated PLL-g-PEG so that the cells had an integrin ligand enabling attachment only either on the protein-coated UV-exposed 1.5 µm wide lines, or on the 5 µm wide areas between the UV-exposed lines, which were made accessible for the cells with streptavidin-conjugated ligands.

Micropatterned lines (1.5 µm) were coated with either of 15 µg/ml fibronectin or collagen type I (calf skin) and 5 µg/ml BSA-AF555 for visualization. In the other two groups of micropatterns, the micropatterns were visualized with 5 µg/ml BSA-AF555, and the area between the patterns were coated with streptavidin-conjugated ligands, either 5 µg/ml of streptavidin-FNIII(7-10) (fibronectin fragment) or streptavidin-GFOGER. All dilutions were done in PBS. The cover glasses were then blocked with 2 % BSA / PBS for 30 min to prevent nonspecific binding.

MDA-MB-231 cells were seeded on the micropatterns to a target confluency of 20 % and allowed to spread for 3 hours in a cell incubator. The cells were then fixed, and their actin cytoskeleton, DNA/nuclei and IACs were immunofluorescence stained using SiR-Actin, DAPI and an anti-paxillin-antibody.

5.4.3 Comparison of U-251 MG cell cytoskeleton and adhesion sites confined on crossbow shaped micropatterns on conventional PLL-g-PEG and biotinylated PLL-g-PEG

U-251MG cells were seeded onto 37 µm wide crossbow-shaped micropatterns on conventional PLL-g-PEG and biotinylated-PLL-g-PEG, which were coated with matrix protein fibronectin (15 µg / ml), and AF-647-conjugated fibrinogen (5 µg / ml) for visualization of the micropatterns. The cells were allowed to spread for 3 h in the cell incubator before fixing and immunofluorescence staining. The cells were then fixed, and their actin cytoskeleton, DNA/nuclei and IAC adhesion sites were immunofluorescence stained using phalloidin-488, DAPI and an anti-paxillin-antibody.

To observe and compare the actin cytoskeleton mean distribution and mean adhesion site localization of the cells on conventional PLL-g-PEG and biotinylated PLL-g-PEG, the images were reoriented and aligned based on the visualized micropatterns to overlay the cells of each group. Thereafter, average intensity projections of actin and paxillin channels were created over the stacks of overlaid cells. These “average cells” were then presented both as grayscale projections and color-coded heatmaps.

5.5 Cell front-rear polarization on different integrin ligands

5.5.1 Tracking cell polarization of fixed U-251 MG cells on static micropatterns

Crossbow-shaped micropatterns were coated with 50 µg / ml of each substrate of interest, including fibronectin, collagen type I, vitronectin (thVTN-N), laminin-521 (LN-521), mAb13 and 12G10, and additionally 5 µg / ml BSA-555 for visualizing the patterns. U-251 MG cells were seeded on the micropatterns and allowed to attach and spread for 3 h before fixing and immunofluorescence staining of the samples. Immunofluorescence staining was used to visualize their actin cytoskeleton, DNA/nuclei, IACs and centrosome (MTOC), using phalloidin-488, DAPI, anti-paxillin-antibody and γ-tubulin-antibody, respectively. The micropatterns were blocked with anti-mouse-AF555 antibody at 1:200 for approximately 1 h

at RT before primary antibody incubation to prevent the secondary anti-mouse antibodies from binding to 12G10 coating.

Images were analyzed using ImageJ/Fiji v1.52 or newer. The images were rotated so that the micropatterns were pointing up. A custom macro was used for data organization and recording the obtained coordinates in automatic segmenting of the nuclei and manual detection of the centrosomes. The coordinate data was combined, and the nucleus – centrosome vectors were calculated in RStudio and drawn with GeoGebra, presented as the centroid of the nucleus being the origo. Circular histograms of the nucleus – centrosome vector angles, were created using Georose 0.5.1. Data was binned in groups of 30 °.

5.5.1 Tracking cell polarization and migration with live-imaging

Crossbow-shaped micropatterns were coated with 50 µg/ml of fibronectin or mAb13 and 5 µg/ml of BSA-AF555 for visualization. U-251 MG or MDA-MB-231 cells stably expressing EGFP-centrin-2 (for detection of the centrosomes) were seeded on the micropatterns and allowed to spread for 3 to 4 hours until fully spread. The cell edges were detected from brightfield images, and nuclei were visualized using SPY650-DNA. Any time points where cells collided with others, or started undergoing apoptosis or mitosis were discarded from the analyses.

To study the dynamics of cell polarization on static micropatterns, U-251 MGs and MDA-MB-231 cells were imaged every 5 minutes for 3 hours (37 time points). In the migration experiments with dynamic micropatterns, the cells were imaged every 5 minutes from 10 min before to 60 min after the addition of streptavidin-conjugated fibronectin, and subsequent time points every 15 min.

When studying cell polarization with live-imaging on static micropatterns, the location of centrosome and segmenting the nuclei were recorded with ImageJ, similar to the fixed samples. Again, the coordinate data was combined, and the nucleus – centrosome vectors were calculated in RStudio. Circular histograms of the nucleus – centrosome vector angles were created using Georose 0.5.1. Data was binned in groups of 30 °.

To analyze the migration data, the nuclei were segmented and tracked using CellProfiler v4.2.4 (Broad Institute) with a custom CellProfiler pipeline, whereas cell outlines and centrosomes were detected and tracked using ImageJ. Again, the coordinate data was combined, and the nucleus – centrosome vectors were calculated in RStudio.

5.6 Image acquisition

An EVOS fluorescent microscope (Advanced Microscopy Group) equipped with ICX285AL CCD camera (Sony), and 20x/0.45 NA PlanFluor objective (Advanced Microscopy Group) were used to check the quality of micropatterns mid-experiment before seeding the cells.

Image acquisition of fixed and immunofluorescence-stained samples was carried out with 3i Marianas CSU-W1 Spinning disk (50µm pinholes) confocal microscope equipped with a Hamamatsu sCMOS Orca Flash4.0 camera (Hamamatsu Photonics) using 20x/0.8 NA PlanApochromat (Zeiss), 40x/1.1 NA W LD C-Apochromat (Zeiss), 63x/1.4 NA O Plan-Apochromat (Zeiss) and 100x/1.4 NA O Plan-Apochromat (Zeiss) objectives.

Live-imaging was carried out with Nikon Eclipse Ti2-E 3i CSU-W1 microscope equipped with a Hamamatsu sCMOS Orca Flash4.0 camera using 20x/0.75 Nikon CFI Plan Apo Lambda objective or 40x/0.6 NA CFI S Plan Fluor ELWD ADM (Nikon) without immersion. All live-cell imaging was performed in a humidified incubator (Okolab) at +37°C, 5% CO2.

5.7 Quantification and statistical analysis

Statistical analyses were performed using GraphPad Prism v.6.05 (GraphPad), Excel and R v.3.5.1 (R Core Team) running on RStudio v.1.3.1073. P value 0.05 or less was considered statistically significant. The names and/or numbers of individual statistical tests, samples and data points are indicated in figure legends.

No strategy was employed for randomization and/or stratification. No blinding or sample-size estimations were performed at any stage of the study.

5.8 Western blotting

5.8.1 Preparation of protein samples

6-well polystyrene (PS) plates were coated with integrin ligands / anti-integrin antibodies by incubating them in 1,5 ml of 20 µg / ml FN, Col type I, 12G10 or mAb13 for 2 h at +37 °C. The protein-coated wells were washed three times with sterile PBS, blocked with 2 % BSA / PBS for 15 min and again washed with PBS. The plates were filled with cell culture medium, allowed to equilibrate to +37 °C in a cell culture incubator and used for experimenting the same day.

The cells were seeded to a confluence of 80 – 100 % without (starved) and in the presence of fibronectin-depleted FBS and were left to attach and spread for 30 min in a cell culture incubator before collecting the cell lysates.

To collect the protein samples, the cells were placed on ice, rinsed twice with ice-cold PBS and lysed with TXLB lysis buffer containing 50 mM Tris-HCl pH 7.5, 150 mM NaCl, 1% SDS, 0.5% Triton X-100, 5% glycerol, and protease (Roche, 05056489001) and phosphatase (Roche, 04906837001) inhibitors. The cell samples were then scraped to microcentrifuge tubes with cell scrapers, incubated at 90 °C for 10 min, centrifuged down, and further homogenized by sonication on ice for 5 min. Relative protein concentrations of the samples were measured with Multiskan Ascent spectrophotometer (Thermo Scientific) using DC Protein Assay kit (Bio-Rad), and the samples were diluted in sample buffer to correspond with the sample having the lowest concentration of total protein on the gel.

5.8.2 Gel electrophoresis and immunoblotting

For gel electrophoresis 4%–20% Mini-PROTEAN TGX Precast Protein Gels (Bio-Rad) were used. The proteins were transferred to 0.2 µm nitrocellulose membranes using Trans-Blot Turbo Transfer Pack, mini or midi format (Bio-Rad, #170-4158, #170-4159). An even transfer quality was ensured with Ponceau S staining. The membranes were blocked 30 min in AdvanBlock Fluor (Advansta, R-03729-E10) blocking buffer. Antibody incubations were for primary antibodies overnight at + 2 – +8 °C, and for fluorophore-conjugated secondary antibodies approx. 90 min at RT. All antibody incubations were done in 1:1 AdvanBlock Fluor Solution/ PSB.

The fluorescent secondary antibodies on the membranes were visualized using ChemiDocTM MP Imaging System (Bio-Rad) and band densities were analyzed using ImageJ v.1.52p (National Institutes of Health). Here, Erk 1/2 was detected as one band. Depending on experimental conditions, it can also be separated into two bands (42 & 44 kDa). GAPDH was used to ensure equal loading, but not to normalize the results.

The phosphorylation ratios of FAK, Akt and Erk of U-251 MG cells on Col type I, 12G10 and mAb13 were normalized against phosphorylation ratios of FAK, Akt and Erk of U-251 MG cells on fibronectin. Statistical differences between phosphorylation ratios of cells on fibronectin and cells on other integrin ligands were calculated with Kruskal-Wallis test and

subsequently using Dunn's multiple comparison test. P-value < 0.05 was considered significant (CI 95 %).

5.9 Data and code availability

Data and code are available on reasonable request from the principal supervisor.

6 Acknowledgements

I want to acknowledge:

Johanna Ivaska for the idea of utilizing biotinylated PLL-g-PEG and streptavidin-conjugated integrin ligands for dynamic micropatterning and the opportunity to continue the previous work of the lab to optimize and validate the method, especially the work of Aleksi Isomursu. Also, I want to acknowledge both Johanna Ivaska and Aleksi Isomursu for their guidance and support through this project. You both have been inspiring role models with genuine enthusiasm for cell research.

The Cell Imaging and Cytometry (CIC) Core facilities (Turku Bioscience Centre, University of Turku and Åbo Akademi University) supported by Biocenter Finland for providing well-maintained imaging equipment for research purposes and professional support and help in their usage.

Teachers of Drug Discovery and Development in Master's Degree Programme in Biomedical Sciences for giving me this opportunity to challenge myself and to develop my academic research skills.

7 Abbreviations

FAK	Focal adhesion kinase
IAC	Integrin adhesion complex
PLL-g-PEG	poly(l-lysine)-graft-poly(ethylene glycol)

References

Abercrombie. 1970. The locomotion of fibroblasts in culture. Experimental Cell Research 59 (393-398).

Abercrombie. 1978. The crawling movement of metazoan cells. Proc. R . Soc. Lond. B 207 (129-147). https://royalsocietypublishing.org/

Alberts B, Johnson A, Lewis J, Raff M, Roberts K, Walter P. 2008. Molecular Biology of the Cell. Garland Science.

Alday-Parejo B, Stupp R, Rüegg C. 2019. Are Integrins Still Practicable Targets for Anti-Cancer Therapy? Cancers (Basel) 11(7):978.

Asati V, Mahapatra DK, Bharti SK. 2016. PI3K/Akt/mTOR and Ras/Raf/MEK/ERK signaling pathways inhibitors as anticancer agents: Structural and pharmacological perspectives. European Journal of Medicinal Chemistry 109:314–341.

Bachmann M, Kukkurainen S, Hytönen VP, Wehrle-Haller B. 2019. Cell Adhesion by Integrins. Physiological Reviews 99(4):1655–1699.

Bergert M, Chandradoss SD, Desai RA, Paluch E. 2012. Cell mechanics control rapid transitions between blebs and lamellipodia during migration. Proceedings of the National Academy of Sciences 109(36):14434–14439.

Biswas A, Saha A, Jana B, Kurkute P, Mondal G, Ghosh S. 2013. A Biotin Micropatterned Surface Generated by Photodestruction Serves as a Novel Platform for Microtubule Organisation and DNA Hybridisation. ChemBioChem 14(6):689–694.

Byron A, Humphries JD, Askari JA, Craig SE, Mould AP, Humphries MJ. 2009. Anti-integrin monoclonal antibodies. Journal of Cell Science 122(22):4009–4011.

Carter SB. 1967. Haptotactic islands: A method of confining single cells to study individual cell reactions and clone formation. Experimental Cell Research 48(1):189–193.

Chastney MR, Conway JRW, Ivaska J. 2021. Integrin adhesion complexes. Curr Biol 31(10):R536–R542.

Children's Hospital Los Angeles. 2023. Study of MEK162 for Children With Low-Grade Gliomas. ClinicalTrials.gov identifier NCT02285439. https://clinicaltrials.gov/study/NCT02285439. Accessed September 28, 2024.

Conway JRW, Jacquemet G. 2019. Cell matrix adhesion in cell migration. Essays in Biochemistry 63(5):535–551.

Cully M. 2020. Integrin-targeted therapies branch out. Nat Rev Drug Discov 19(11):739–741.

Daley WP, Peters SB, Larsen M. 2008. Extracellular matrix dynamics in development and regenerative medicine. Journal of Cell Science 121(3):255–264.

D'Arcangelo E, McGuigan AP. 2015. Micropatterning strategies to engineer controlled cell and tissue architecture in vitro. BioTechniques 58(1):13–23.

Degot S, Auzan M, Chapuis V, Béghin A, Chadeyras A, Nelep C, Calvo-Muñoz ML, Young J, Chatelain F, Fuchs A. 2010. Improved Visualization and Quantitative Analysis of Drug Effects Using Micropatterned Cells. JoVE (Journal of Visualized Experiments) (46):e2514.

Dhillon S. 2022. Carotegrast Methyl: First Approval. Drugs 82(9):1011–1016.

Dubois F, Alpha K, Turner CE. 2017. Paxillin regulates cell polarization and anterograde vesicle trafficking during cell migration. Mol Biol Cell 28(26):3815–3831.

Elbert DL, Hubbell JA. 1998. Self-assembly and steric stabilization at heterogeneous, biological surfaces using adsorbing block copolymers. Chemistry & Biology 5(3):177–183.

Ellert-Miklaszewska A, Poleszak K, Pasierbinska M, Kaminska B. 2020. Integrin Signaling in Glioma Pathogenesis: From Biology to Therapy. International Journal of Molecular Sciences 21(3):888.

Emory University. 2024. Identification of Treatment Concentrations of Defactinib or VS-6766 for the Treatment of Patients With Glioblastoma . ClinicalTrials.gov identifier NCT05798507. https://clinicaltrials.gov/study/NCT05798507. Accessed September 28, 2024.

Erices JI, Bizama C, Niechi I, Uribe D, Rosales A, Fabres K, Navarro-Martínez G, Torres Á, San Martín R, Roa JC, Quezada-Monrás C. 2023. Glioblastoma Microenvironment and Invasiveness: New Insights and Therapeutic Targets. Int J Mol Sci 24(8):7047.

Fink J, Théry M, Azioune A, Dupont R, Chatelain F, Bornens M, Piel M. 2007. Comparative study and improvement of current cell micro-patterning techniques. Lab Chip 7(6):672–680.

Frantz C, Stewart KM, Weaver VM. 2010. The extracellular matrix at a glance. J Cell Sci 123(24):4195–4200.

Friedl P, Wolf K. 2003. Tumour-cell invasion and migration: diversity and escape mechanisms. Nat Rev Cancer 3(5):362–374.

Gressett TE, Nader D, Robles JP, Buranda T, Kerrigan SW, Bix G. 2022. Integrins as Therapeutic Targets for SARS-CoV-2. Front Cell Infect Microbiol 12:892323.

Hesse M, Magin TM, Weber K. 2001. Genes for intermediate filament proteins and the draft sequence of the human genome: novel keratin genes and a surprisingly high number of pseudogenes related to keratin genes 8 and 18. Journal of Cell Science 114(14):2569–2575.

Hohmann T, Dehghani F. 2019. The Cytoskeleton-A Complex Interacting Meshwork. Cells 8(4):362.

Hu H-H, Wang S-Q, Shang H-L, Lv H-F, Chen B-B, Gao S-G, Chen X-B. 2024. Roles and inhibitors of FAK in cancer: current advances and future directions. Front Pharmacol 15.

Huhtala M, Heino J, Casciari D, Luise A de, Johnson MS. 2005. Integrin evolution: insights from ascidian and teleost fish genomes. Matrix Biol 24(2):83–95.

Humphries JD, Schofield NR, Mostafavi-Pour Z, Green LJ, Garratt AN, Mould AP, Humphries MJ. 2005. Dual functionality of the anti-beta1 integrin antibody, 12G10, exemplifies agonistic signalling from the ligand binding pocket of integrin adhesion receptors. J Biol Chem 280(11):10234–10243.

Humphries MJ, Symonds EJ, Mould AP. 2003. Mapping functional residues onto integrin crystal structures. Current Opinion in Structural Biology 13(2):236–243.

InxMed (Shanghai) Co., Ltd. 2024. a Study to Evaluate the Safety and Efficacy of D-1553 Combined With IN10018 in KRAS G12C Mutant Solid Tumors. ClinicalTrials.gov identifier NCT06166836. https://clinicaltrials.gov/study/NCT06166836. Accessed September 28, 2024.

Insua-Rodríguez J, Oskarsson T. 2016. The extracellular matrix in breast cancer. Advanced Drug Delivery Reviews 97:41–55.

Isomursu A, Alanko J, Hernández-Pérez S, Saukkonen K, Saari M, Mattila PK, Ivaska J. 2024. Dynamic Micropatterning Reveals Substrate-Dependent Differences in the Geometric Control of Cell Polarization and Migration. Small Methods 8(1):2300719.

Järveläinen H, Sainio A, Koulu M, Wight TN, Penttinen R. 2009. Extracellular Matrix Molecules: Potential Targets in Pharmacotherapy. Pharmacol Rev 61(2):198–223.

Jiang X, Bruzewicz DA, Wong AP, Piel M, Whitesides GM. 2005. Directing cell migration with asymmetric micropatterns. PNAS 102(4):975–978.

Jokinen E, Laurila N, Koivunen JP. 2012. Alternative dosing of dual PI3K and MEK inhibition in cancer therapy. BMC Cancer 12(1):612.

Kanchanawong P, Calderwood DA. 2023. Organisation, dynamics and mechanoregulation of integrin-mediated cell–ECM adhesions. Nat Rev Mol Cell Biol 24(2):142–161.

Katoh K. 2020. FAK-Dependent Cell Motility and Cell Elongation. Cells 9(1):192.

Koshy M, Villano JL, Dolecek TA, Howard A, Mahmood U, Chmura SJ, Weichselbaum RR, McCarthy BJ. 2012. Improved survival time trends for glioblastoma using the SEER 17 population-based registries. J Neurooncol 107(1):207–212.

LaFoya B, Munroe JA, Miyamoto A, Detweiler MA, Crow JJ, Gazdik T, Albig AR. 2018. Beyond the Matrix: The Many Non-ECM Ligands for Integrins. International Journal of Molecular Sciences 19(2):449.

Lauffenburger DA, Horwitz AF. 1996. Cell Migration: A Physically Integrated Molecular Process. Cell 84(3):359–369.

Li J, Jo MH, Yan J, Hall T, Lee J, López-Sánchez U, Yan S, Ha T, Springer TA. 2024. Ligand binding initiates single-molecule integrin conformational activation. Cell 187(12):2990-3005.e17.

Mahmud G, Campbell CJ, Bishop KJM, Komarova YA, Chaga O, Soh S, Huda S, Kandere-Grzybowska K, Grzybowski BA. 2009. Directing cell motions on micropatterned ratchets. Nature Phys 5(8):606–612.

Martin M, Veloso A, Wu J, Katrukha EA, Akhmanova A. 2018. Control of endothelial cell polarity and sprouting angiogenesis by non-centrosomal microtubules. eLife 7:e33864.

Michael M, Parsons M. 2020. New perspectives on integrin-dependent adhesions. Curr Opin Cell Biol 63:31–37.

Mould AP, Garratt AN, Askari JA, Akiyama SK, Humphries MJ. 1995. Identification of a novel anti-integrin monoclonal antibody that recognises a ligand-induced binding site epitope on the β1 subunit. FEBS Letters 363(1–2):118–122.

Mustafa M, Abd El-Hafeez AA, Abdelhafeez DA, Abdelhamid D, Mostafa YA, Ghosh P, Hayallah AM, A Abuo-Rahma GE-D. 2021. FAK inhibitors as promising anticancer targets: present and future directions. Future Medicinal Chemistry 13(18):1559–1590.

Nakanishi J, Takarada T, Yamaguchi K, Maeda M. 2008. Recent advances in cell micropatterning techniques for bioanalytical and biomedical sciences. Anal Sci 24(1):67–72.

Nobes CD, Hall A. 1999. Rho GTPases control polarity, protrusion, and adhesion during cell movement. J Cell Biol 144(6):1235–1244.

Oppel F, Müller N, Schackert G, Hendruschk S, Martin D, Geiger KD, Temme A. 2011. SOX2-RNAi attenuates S-phase entry and induces RhoA-dependent switch to protease-independent amoeboid migration in human glioma cells. Molecular Cancer 10(1):137.

Paluch EK, Raz E. 2013. The role and regulation of blebs in cell migration. Current Opinion in Cell Biology 25(5):582–590.

Pang X, He X, Qiu Z, Zhang H, Xie R, Liu Z, Gu Y, Zhao N, Xiang Q, Cui Y. 2023. Targeting integrin pathways: mechanisms and advances in therapy. Sig Transduct Target Ther 8(1):1–42.

Pang X-J, Liu X-J, Liu Y, Liu W-B, Li Y-R, Yu G-X, Tian X-Y, Zhang Y-B, Song J, Jin C-Y, Zhang S-Y. 2021. Drug Discovery Targeting Focal Adhesion Kinase (FAK) as a Promising Cancer Therapy. Molecules 26(14):4250.

Pollard TD. 2016. Actin and Actin-Binding Proteins. Cold Spring Harb Perspect Biol 8(8):a018226.

Raudenská M, Petrláková K, Juriňáková T, Fialová JL, Fojtů M, Jakubek M, Rösel D, Brábek J, Masařík M. 2023. Engine shutdown: migrastatic strategies and prevention of metastases. Trends in Cancer 9(4):293–308.

Rotty JD, Bear JE. 2015. Competition and collaboration between different actin assembly pathways allows for homeostatic control of the actin cytoskeleton. Bioarchitecture 5(1–2):27–34.

Salomaa S. 2020. Crosstalk between cell adhesion and the actin cytoskeleton.

Sarkar A, LeVine DN, Kuzmina N, Zhao Y, Wang X. 2020. Cell Migration Driven by Self-Generated Integrin Ligand Gradient on Ligand-Labile Surfaces. Current Biology 30(20):4022-4032.e5.

Seetharaman S, Etienne-Manneville S. 2020. Cytoskeletal Crosstalk in Cell Migration. Trends in Cell Biology 30(9):720–735.

Seetharaman S, Vianay B, Roca V, Farrugia AJ, De Pascalis C, Boëda B, Dingli F, Loew D, Vassilopoulos S, Bershadsky A, Théry M, Etienne-Manneville S. 2022. Microtubules tune mechanosensitive cell responses. Nat Mater 21(3):366–377.

Segerer FJ, Röttgermann PJF, Schuster S, Piera Alberola A, Zahler S, Rädler JO. 2016. Versatile method to generate multiple types of micropatterns. Biointerphases 11(1):011005.

Seker-Polat F, Pinarbasi Degirmenci N, Solaroglu I, Bagci-Onder T. 2022. Tumor Cell Infiltration into the Brain in Glioblastoma: From Mechanisms to Clinical Perspectives. Cancers 14(2):443.

SenGupta S, Parent CA, Bear JE. 2021. The principles of directed cell migration. Nat Rev Mol Cell Biol 22(8):529–547.

Shirley M. 2024. PB006: A Natalizumab Biosimilar. Clin Drug Investig 44(5):367–370.

Slack RJ, Macdonald SJF, Roper JA, Jenkins RG, Hatley RJD. 2022. Emerging therapeutic opportunities for integrin inhibitors. Nat Rev Drug Discov 21(1):60–78.

Takada Y, Ye X, Simon S. 2007. The integrins. Genome Biology 8(5):215.

Théry M. 2010. Micropatterning as a tool to decipher cell morphogenesis and functions. Journal of Cell Science 123(24):4201–4213.

Théry M, Racine V, Piel M, Pépin A, Dimitrov A, Chen Y, Sibarita J-B, Bornens M. 2006. Anisotropy of cell adhesive microenvironment governs cell internal organization and orientation of polarity. PNAS 103(52):19771–19776.

Tran B, Rosenthal MA. 2010. Survival comparison between glioblastoma multiforme and other incurable cancers. Journal of Clinical Neuroscience 17(4):417–421.

Tseng Q, Wang I, Duchemin-Pelletier E, Azioune A, Carpi N, Gao J, Filhol O, Piel M, Théry M, Balland M. 2011. A new micropatterning method of soft substrates reveals that different tumorigenic signals can promote or reduce cell contraction levels. Lab on a Chip 11(13):2231–2240.

Wang J, Cai C, Nie D, Song X, Sun G, Zhi T, Li B, Qi J, Zhang J, Chen H, Shi Q, Yu R. 2019. FRK suppresses human glioma growth by inhibiting ITGB1/FAK signaling. Biochemical and Biophysical Research Communications 517(4):588–595.

Watson JL, Aich S, Oller-Salvia B, Drabek AA, Blacklow SC, Chin J, Derivery E. 2021. High-efficacy subcellular micropatterning of proteins using fibrinogen anchors. J Cell Biol 220(2):e202009063.

Weeks A, Okolowsky N, Golbourn B, Ivanchuk S, Smith C, Rutka JT. 2012. ECT2 and RASAL2 Mediate Mesenchymal-Amoeboid Transition In Human Astrocytoma Cells. The American Journal of Pathology 181(2):662–674.

Weems AD, Welf ES, Driscoll MK, Zhou FY, Mazloom-Farsibaf H, Chang B-J, Murali VS, Gihana GM, Weiss BG, Chi J, Rajendran D, Dean KM, Fiolka R, Danuser G. 2023. Blebs promote cell survival by assembling oncogenic signalling hubs. Nature 615(7952):517–525.

Yap FL, Zhang Y. 2007. Protein and cell micropatterning and its integration with micro/nanoparticles assembly. Biosensors and Bioelectronics 22(6):775–788.

You C, Piehler J. 2016. Functional protein micropatterning for drug design and discovery. Expert Opinion on Drug Discovery 11(1):105–119.

Zhong J, Paul A, Kellie SJ, O'Neill GM. 2010. Mesenchymal Migration as a Therapeutic Target in Glioblastoma. Journal of Oncology 2010:e430142.